

Selected Topics in Jet Quenching



Ivan Vitev

In collaboration with Michael Fickinger, Jinrui Huang, Zongbo Kang, Grigory Ovanesyan

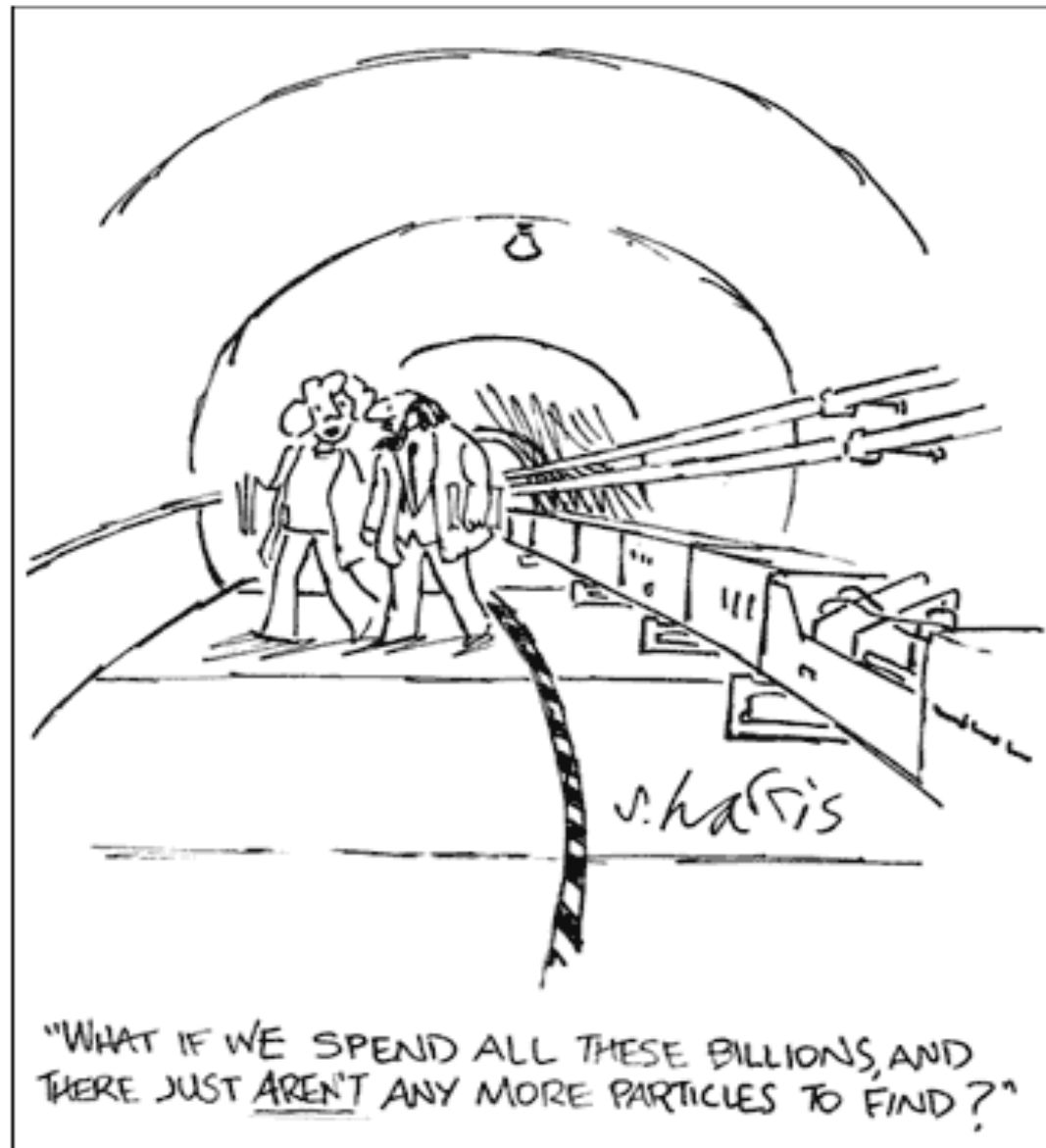
1. ArXiv: 1304.3497 [hep-ph], JHEP 1307 (2013) 059
2. ArXiv: 1306.0909 [hep-ph], Phys. Lett. B in press (2013)

International Workshop on High p_T at the LHC
September 2013, Grenoble, France

Outline of the Talk

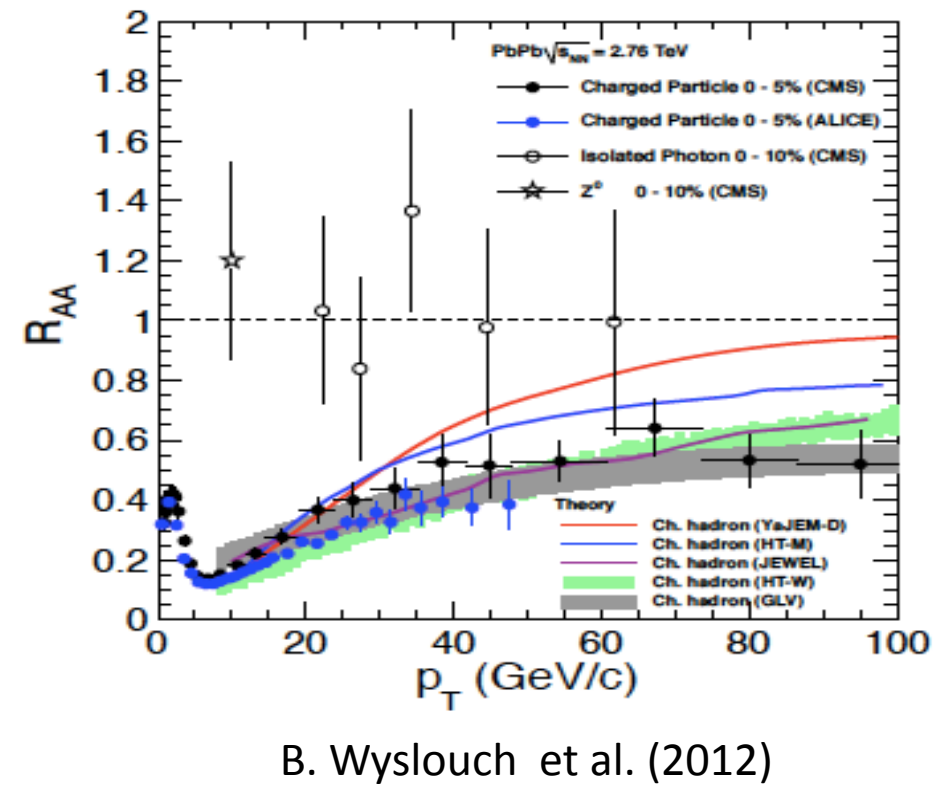
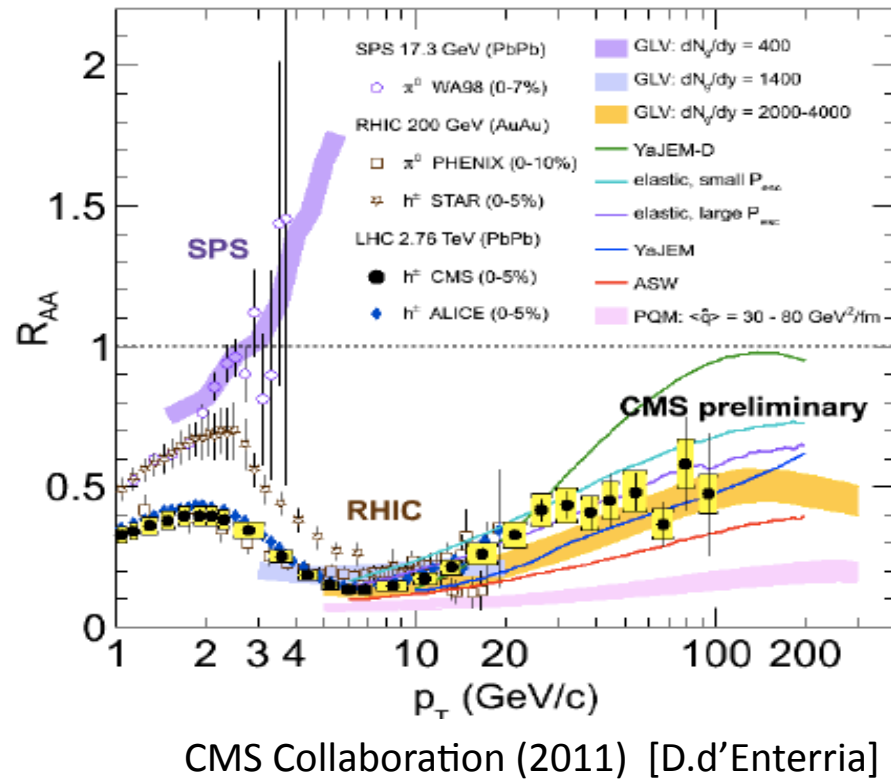
- Introduction: Why do analytic jet cross section calculations and quenching of jets work?
- $SCET_G$. Parton showers. Absence of angular ordering in the collinear parton shower.
- Heavy flavor suppression. Effective heavy degrees of freedom. B-jet quenching.
- Conclusions.

I. Introduction



From leading hadrons to jets

- Similarly to RHIC, first important constraints on jet quenching and data for jet tomography at the LHC have come from leading particle suppression



- An important step forward at the LHC is the development of the theory of jets and the now many measurements in A+A

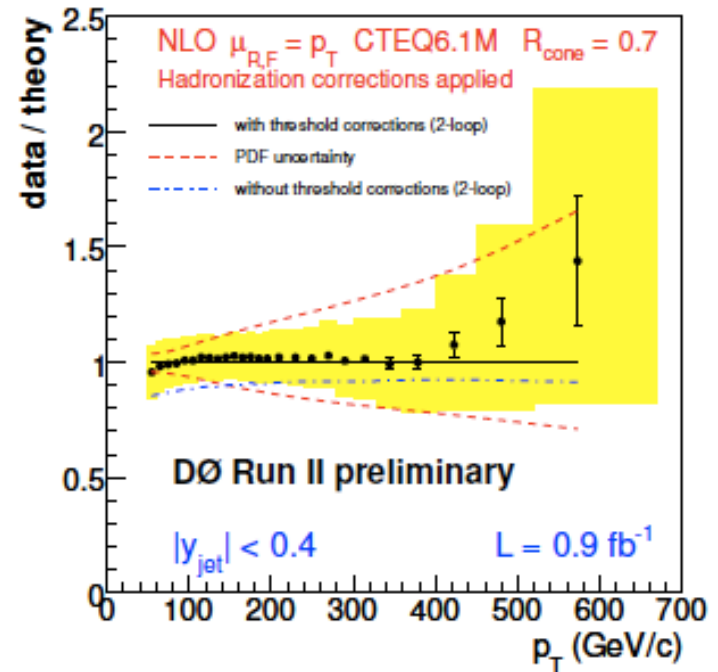
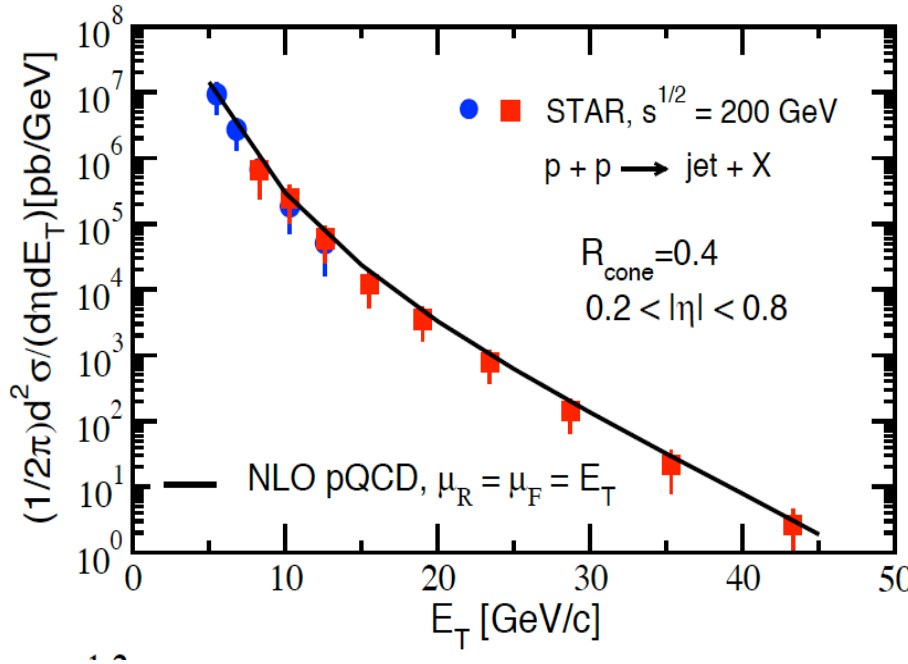
Jet cross sections

- Interestingly, some of the most accurate predictions for inclusive jet observables have come from fixed order NLO calculations

$$\frac{d\sigma^{\text{jet}}}{dE_T dy} = \frac{1}{2!} \int d\{E_T, y, \phi\}_2 \frac{d\sigma[2 \rightarrow 2]}{d\{E_T, y, \phi\}_2} S_2(\{E_T, y, \phi\}_2) + \frac{1}{3!} \int d\{E_T, y, \phi\}_3 \frac{d\sigma[2 \rightarrow 3]}{d\{E_T, y, \phi\}_3} S_3(\{E_T, y, \phi\}_3)$$

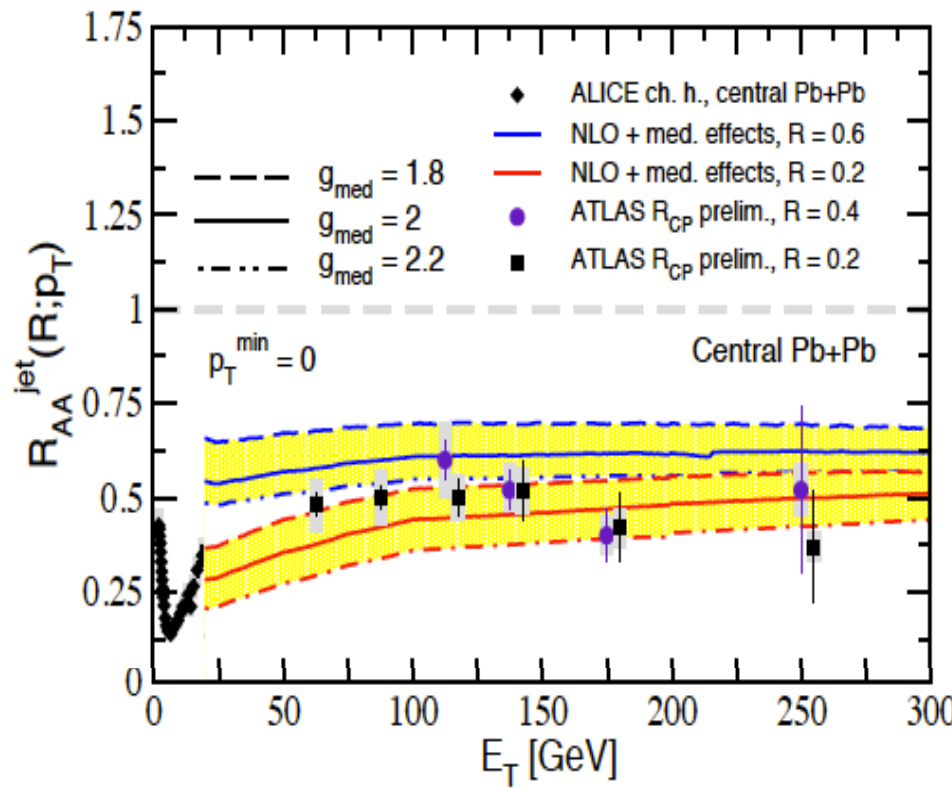
S.D. Ellis et al (1990)

Z. Kunszt et al (1992)

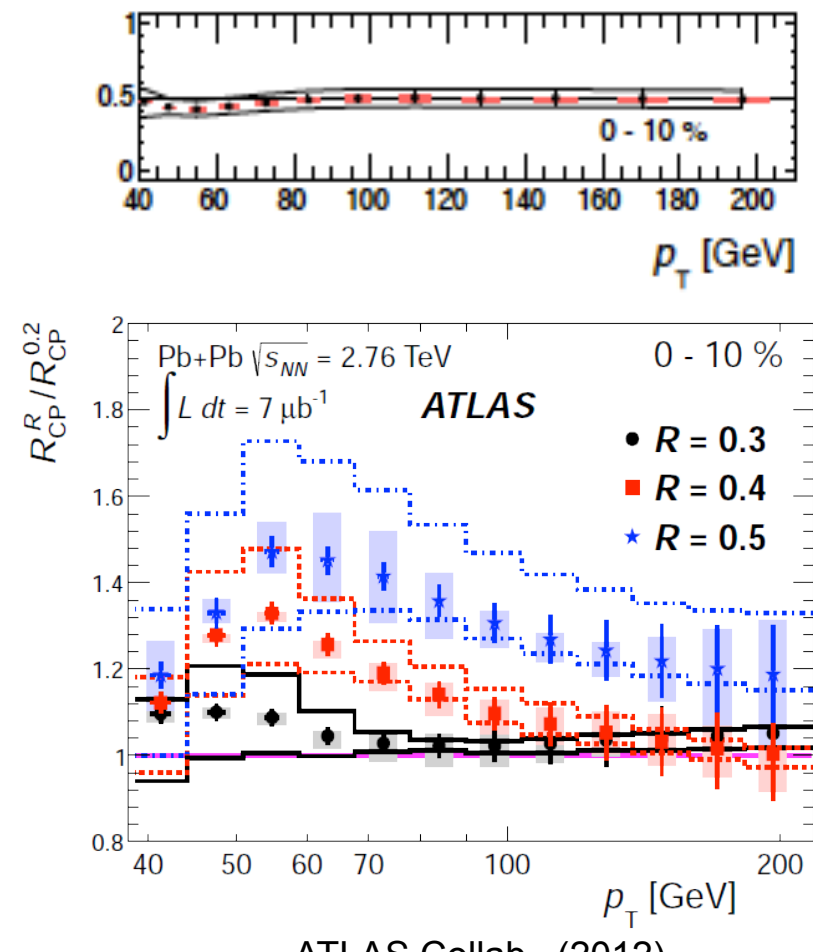


Medium-modified jet cross sections

- Similarly, semi-analytic predictions for modification of jet observables compare favorably to LHC data



Y. He et al. (2011)



ATLAS Collab. (2012)

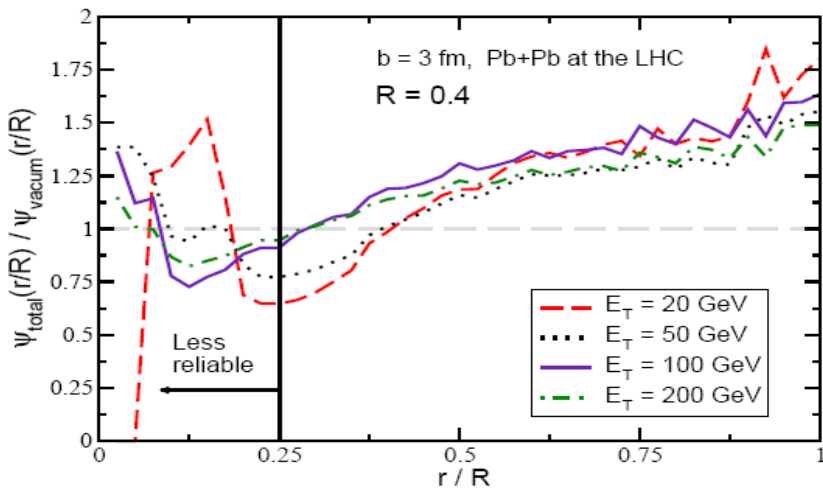
Intra-jet observables

$$\Psi_{\text{int}}(r; R) = \frac{\sum_i (E_T)_i \Theta(r - (R_{\text{jet}})_i)}{\sum_i (E_T)_i \Theta(R - (R_{\text{jet}})_i)},$$

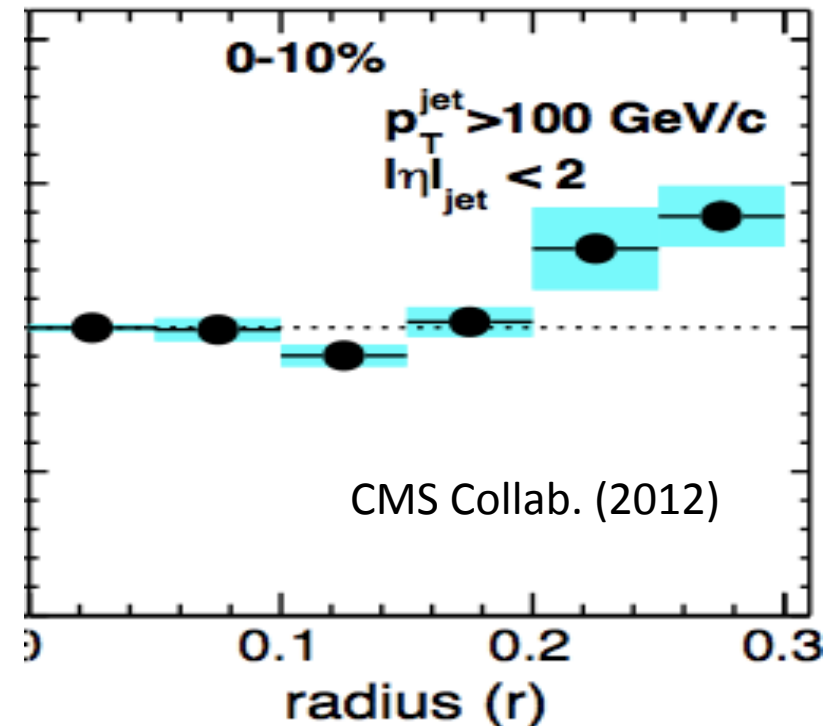
$$\psi(r; R) = \frac{d\Psi_{\text{int}}(r; R)}{dr}.$$

R=0.4	Vacuum	Complete E-loss	Realistic Case
$\langle r/R \rangle, E_T = 20 \text{ GeV}$	0.41	0.57	0.45
$\langle r/R \rangle, E_T = 50 \text{ GeV}$	0.35	0.53	0.38
$\langle r/R \rangle, E_T = 100 \text{ GeV}$	0.28	0.42	0.32
$\langle r/R \rangle, E_T = 200 \text{ GeV}$	0.25	0.42	0.28

I. Vitev et al. (2008)



- There is no big difference between the average jet shape in vacuum and the total jet shape in the medium
- Take a ratio of the differential jet shapes

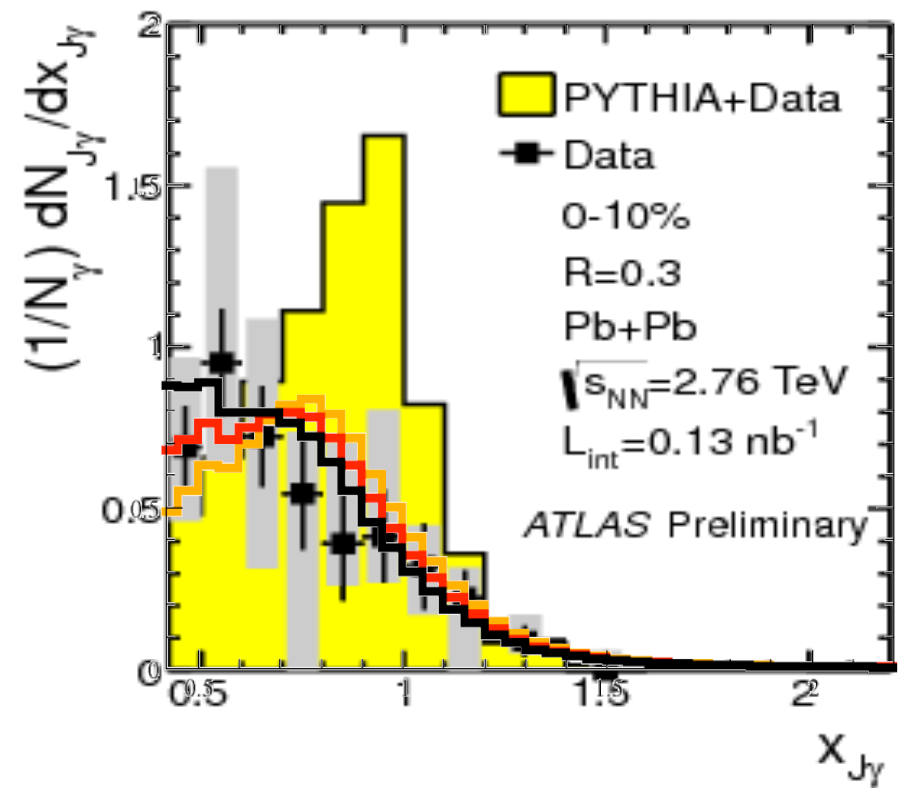
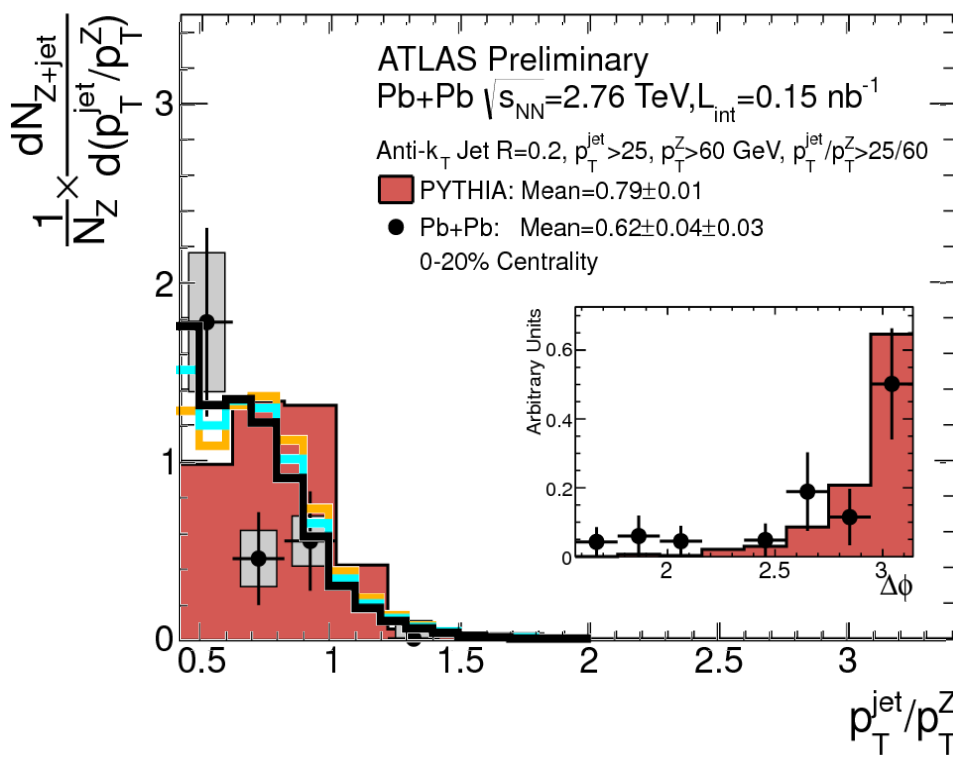


Photon-tagged and Z⁰-tagged jets

Imbalance variable $Z_J = \frac{p_{T\ jet}}{p_{T\ \gamma}}$

$$\frac{d\sigma}{dz_{J\gamma}} = \int_{p_{T\text{jet}}^{\min}}^{p_{T\text{jet}}^{\max}} dp_{T\text{jet}} \frac{p_{T\text{jet}}}{z_{J\gamma}^2} \frac{d\sigma[z_{J\gamma}, p_{T\gamma}(z_{J\gamma}, p_{T\text{jet}})]}{dp_{T\gamma} dp_{T\text{jet}}}$$

- Taken directly from the QM 2012 jet highlights



The Original Snowmass Accord

- Tried to put some order in the rapidly developing field of jet physics (disconnect between different measurements, between measurements and theory ...).

A lot of the “practical output” has failed

The cone algorithm turned out to not be collinear and infrared safe at higher order

On the other hand, the accord for theory lives on and its implications can be seen in the comparison to the LHC measurements

- a) Observables should be infrared and collinear safe
- b) They should not be sensitive to hadronization corrections
- c) Jet measurements should reflect the QCD dynamic at the perturbative scale

II. Absence of angular ordering



What does a parton shower do?

- The most accurate calculations in hadronic collisions are fixed order and/or matched to resummation
- Parton shower Monte Carlos can address exclusive and complex final states at the expense of multiple approximations

Markov process with probabilities to:

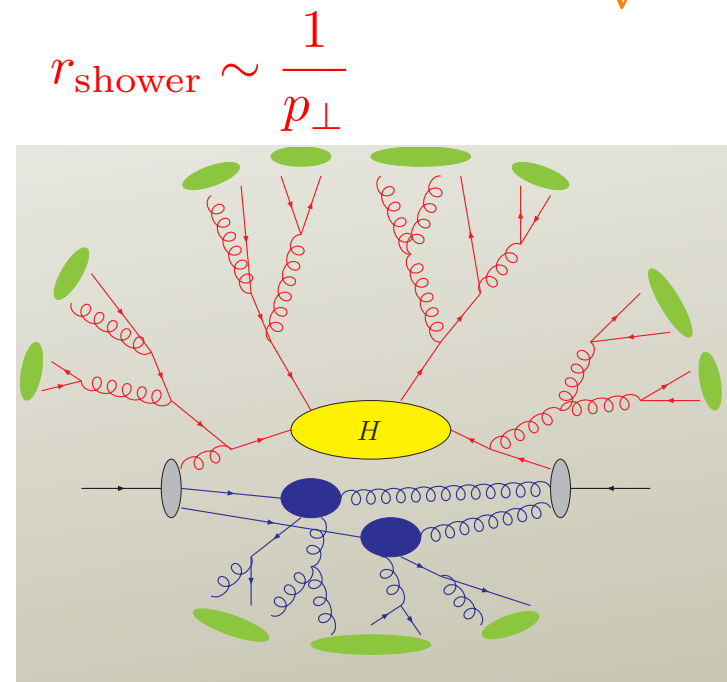
- Knock a parton out of the proton (PDF)
- Collinear splittings (radiation)
- Hadronization

$$r_{\text{soft}} \sim \frac{1}{\Lambda_{\text{QCD}}}$$

$$r_{\text{hard}} \sim \frac{1}{\sqrt{s}}$$

Parton Shower includes resummation of Sudakov logarithms (leading)

In this talk we focus on the properties of collinear splittings in the vacuum and in the dense matter



Altarelli-Parisi splitting functions versus coherent branching

$$r_{\text{shower}} \sim \frac{1}{p_\perp}$$

E_0 $E_0(1 - z)$

$E_0 z$

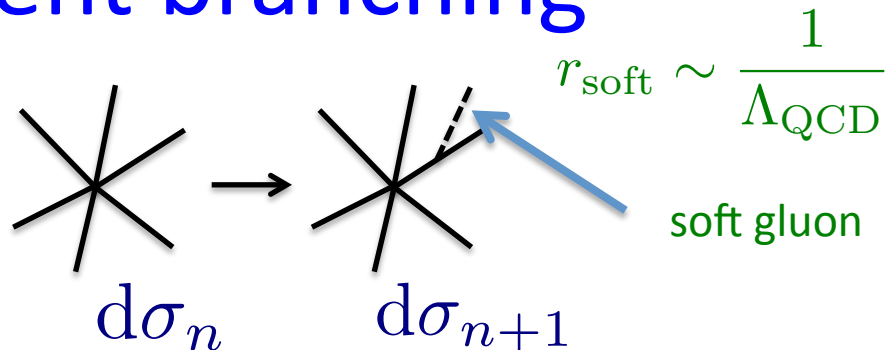
collinear parton

$|\mathcal{M}_{a_1, a_2, \dots}(p_1, p_2, \dots)|^- \simeq$

$$\frac{2}{s_{12}} 4\pi\mu^{2\epsilon} \alpha_S \mathcal{T}_{a, \dots}^{ss'}(p, \dots) \hat{P}_{a_1 a_2}^{ss'}(z, k_\perp; \epsilon)$$

- Comes at the scale of **collinear radiation** inside the parton shower
- Factorize and are process independent

Coherence branching effects incorporated into splitting functions,
HERWIG - a Monte Carlo generator for parton showers



$$d\sigma_{n+1} = d\sigma_n \frac{d\omega}{\omega} \frac{d\Omega}{2\pi} \frac{\alpha_S}{2\pi} \sum_i C_{ij} W_{ij}$$

W_{ij} is the antenna function that leads to angular ordering

$$W_{ij} = \frac{\omega^2 p_i \cdot p_j}{p_i \cdot q p_j \cdot q} = \frac{1 - \cos \theta_{ij}}{(1 - \cos \theta_{iq})(1 - \cos \theta_{jq})}$$

- Comes from the physics at the **soft scale**
- At **soft (long distance)** scales the emissions are **angular ordered**

Why is this calculation possible?

- Modes in SCET

Energetic quarks and leptons
collinear modes

Include also soft quarks and gluons

C. Bauer et al. (2001)

D. Pirol et al. (2004)

$$p_c = (p_+, p_-, p_\perp) \sim \left(\frac{\Lambda^2}{Q}, Q, \Lambda \right) = Q(\lambda^2, 1, \lambda)$$

$$p_s = (p_+, p_-, p_\perp) \sim (\Lambda, \Lambda, \Lambda) = Q(\lambda, \lambda, \lambda)$$

Collinear quarks, antiquarks	$\xi_n, \bar{\xi}_n$
Collinear gluons, soft gluons	A_n, A_s

Soft quarks are eliminated through the equations of motion or integrated out in the QCD action

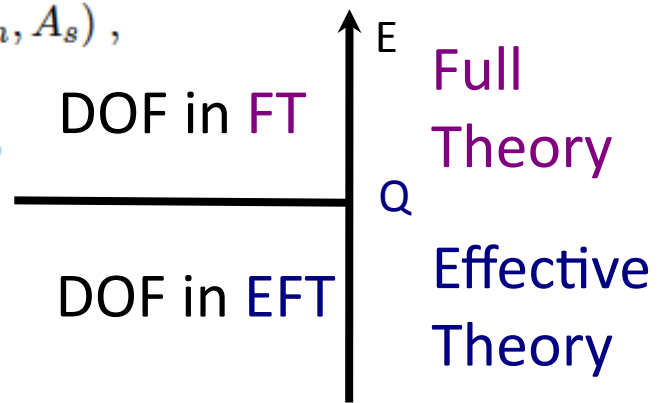
- SCET Lagrangian to all orders in λ [Can expand to LO, NLO,...]

$$\mathcal{L}_{\text{SCET}}(\xi_n, A_n, A_s) = \bar{\xi}_n \left[i n \cdot D + i \not{D}^\perp \frac{1}{i \bar{n} \cdot D} i \not{D}^\perp \right] \frac{\not{n}}{2} \xi_n + \mathcal{L}_{\text{YM}}(A_n, A_s),$$

$$\mathcal{L}_{\text{YM}}(A_n, A_s) = \frac{1}{2g^2} \text{tr} \{ [iD_s^\mu + gA_{n,q}^\mu, iD_s^\nu + gA_{n,q'}^\nu] \}^2 + \mathcal{L}_{\text{G.F.}},$$

$$\mathcal{L}_{\text{G.F.}}(R_\xi) = \frac{1}{\xi} \text{tr} \{ [iD_{s\mu}, A_{n,q}^\mu] \}^2,$$

$$\mathcal{L}_{\text{G.F.}}(\text{LCG}(b)) = \frac{1}{\xi} \text{tr} \{ b_\mu A_{n,q}^\mu \}^2.$$



SCET with Glauber gluons

- Galuber gluons (transverse to the jet direction)

A. Idilbi et al. (2009)

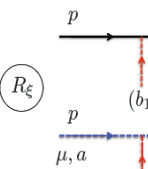
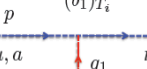
$$q \sim [\lambda^2, \lambda^2, \lambda]$$

$$\mathcal{L}_{\text{SCET}_G}(\xi_n, A_n, A_G) = \mathcal{L}_{\text{SCET}}(\xi_n, A_n) + \mathcal{L}_G(\xi_n, A_n, A_G)$$

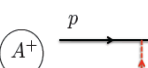
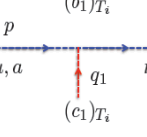
G. Ovanesyan et al. (2011)

$$\mathcal{L}_G(\xi_n, A_n, \eta) = \sum_{p, p', q} e^{-i(p-p'+q)x} \left(\bar{\xi}_{n,p'} \Gamma_{\text{qqA}_G}^{\mu,a} \frac{\not{q}}{2} \xi_{n,p} - i \Gamma_{\text{ggA}_G}^{\mu\nu\lambda,abc} (A_{n,p'}^c)_\lambda (A_{n,p}^b)_\nu \right) \bar{\eta} \Gamma_s^{\delta,a} \eta \Delta_{\mu\delta}(q)$$

- Complete Feynman rules in the soft, collinear and hybrid gauges

	$= i v(q_{1\perp}) (b_1)_R (b_1)_{T_i} \frac{\not{q}}{2}$
	$= v(q_{1\perp}) f^{abci} (c_1)_{T_i} \left[g^{\mu\nu} \bar{n} \cdot p + \bar{n}^\mu q_{1\perp}^\nu - \bar{n}^\nu q_{1\perp}^\mu - \frac{1-\xi}{2} (\bar{n}^\nu p^\mu + \bar{n}^\mu p^\nu) \right]$

- First proof of gauge invariance of the broadening/radiative energy loss results

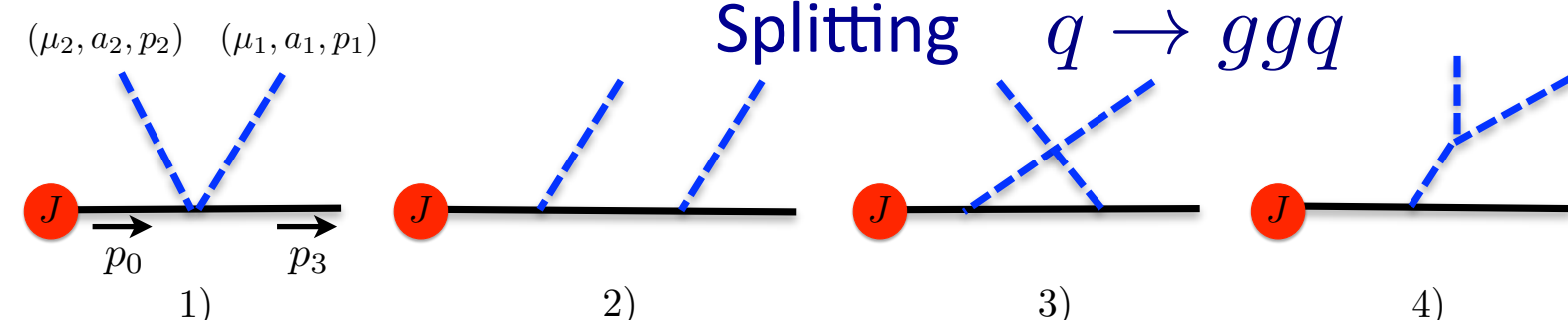
	$= i v(q_{1\perp}) (a)_R (b_1)_{T_i} \left(1 + \frac{p^2 - p'^2}{p^+ [q_1^+]} \right) \frac{\not{q}}{2}$
	$= v(q_{1\perp}) f^{abci} (c_1)_{T_i} \left[g_\perp^{\mu\nu} \bar{n} \cdot p \left(1 + \frac{p^2 - p'^2}{p^+ [q_1^+]} \right) + \frac{q_{1\perp}^\mu p^\nu + q_{1\perp}^\nu p^\mu}{[q_1^+]} \right]$

Many more ...

- Showed factorization of the final-state process-dependent radiative corrections and the hard scattering cross section, calculated large-x

$$\int \frac{d^2 q_\perp}{(2\pi)^2} |\tilde{v}(q_\perp)|^2 \text{Tr} \left(\frac{\not{q}}{2} \bar{n} \cdot p J \bar{J} \frac{g^2}{d_R d_T} [\rho^{\text{SB}} + \rho^{\text{DB}}] \right) \quad \rho = \sum_{i=1}^2 c_i (F_i \mathbb{I} + G_i \Sigma^3)$$

$O(\alpha_s^2)$ splitting functions in the vacuum



$$z_i = E_i / (E_1 + E_2 + E_3)$$

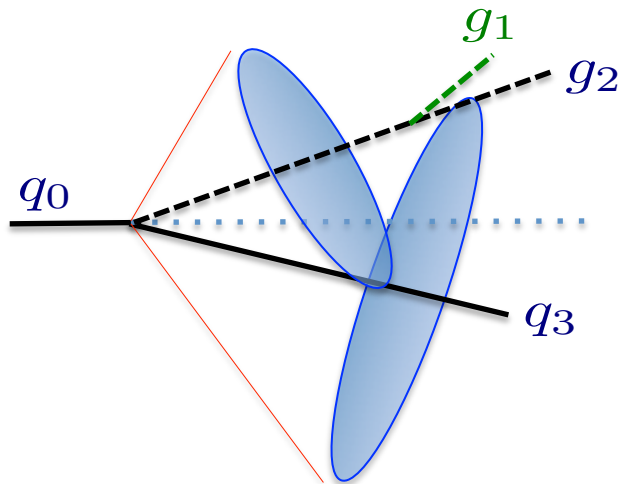
$$s_{ij} = (p_i + p_j)^2$$

$$\langle \hat{P}_{g_1 g_2 q_3} \rangle = C_F^2 \langle \hat{P}_{g_1 g_2 q_3}^{(ab)} \rangle + C_F C_A \langle \hat{P}_{g_1 g_2 q_3}^{(nab)} \rangle$$

- We use the Feynman rules of **SCET**, reproduce Catani-Grazzini's result exactly. Only the collinear sector enters
- Notes Without taking the small z_1 limit, the notion of ordering is **meaningless**

$$\langle P_{g_1 g_2 q_3} \rangle (z_1 \ll z_2, z_3)$$

No radiation outside the cones is an **on average** statement even in the ultrasoft limit



$$W_{23} = W_{23}^{[2]} + W_{23}^{[3]}$$

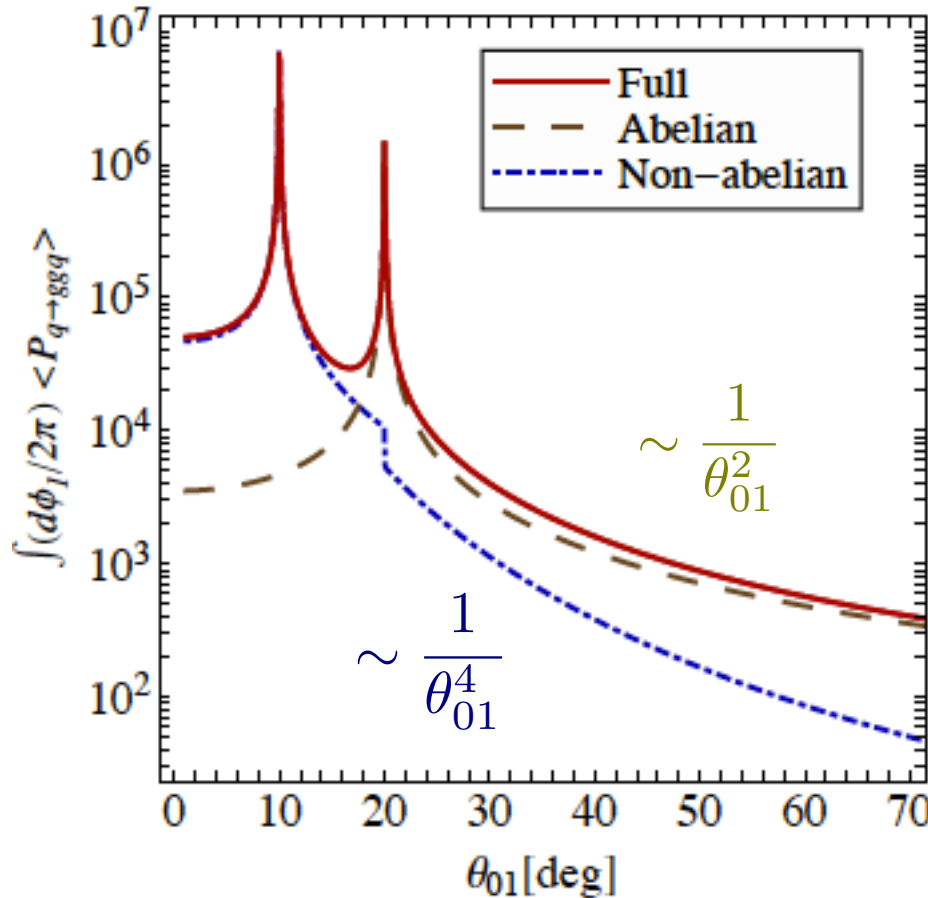
$$\int \frac{d\varphi_{12}}{2\pi} W_{23}^{[2]} = 0 \int \frac{d\varphi_{13}}{2\pi} W_{23}^{[3]} = 0$$

Angular distribution of the vacuum splitting functions

$$z_2 = 2/3 \quad \theta_{20} = 10^\circ, \theta_{30} = 20^\circ$$

$$z_1 = 0.03 \ll z_2, z_3$$

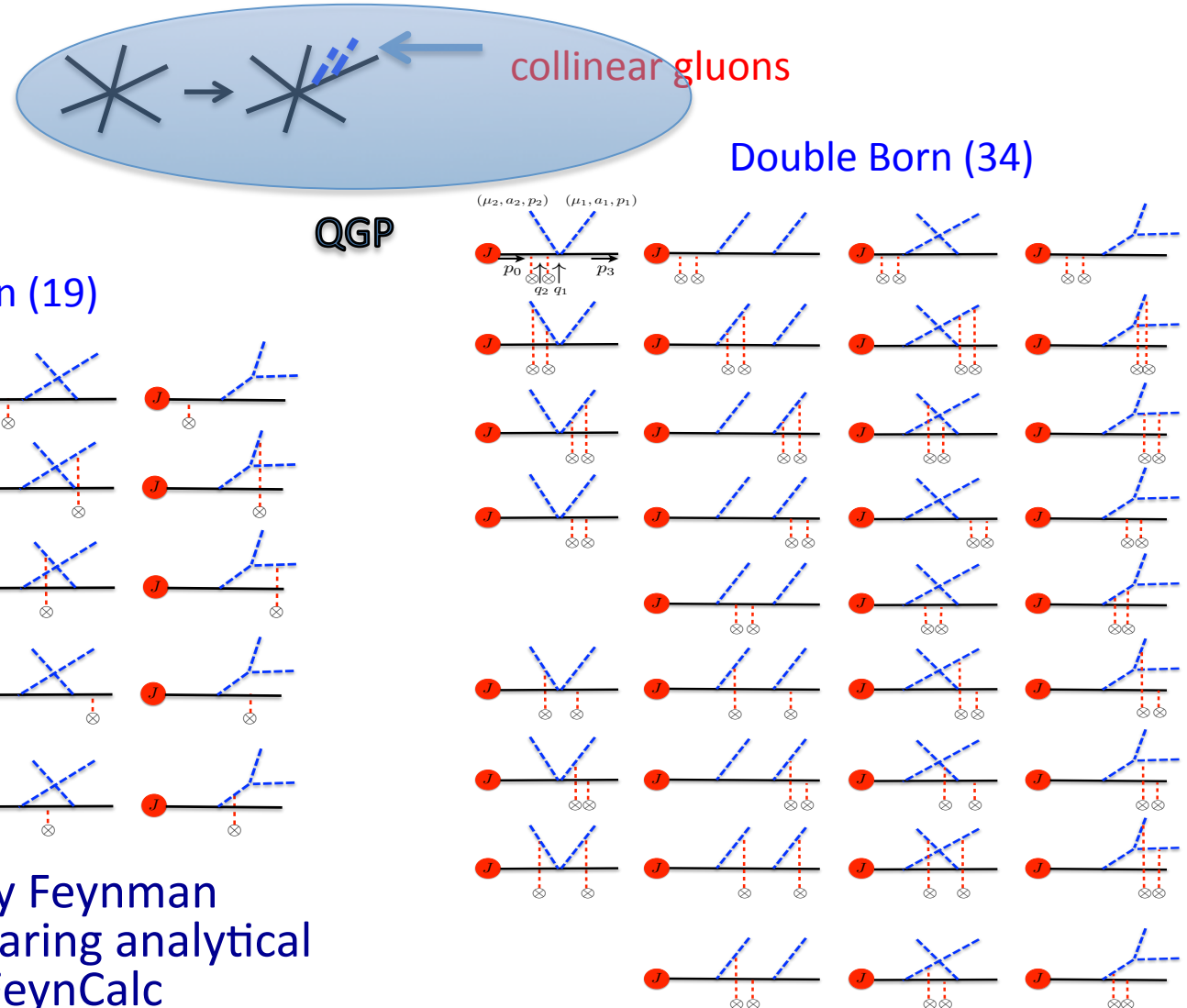
Splitting function $q \rightarrow ggq$



- Scaling $1/\theta^2$ is consistent with **no angular ordering**
 - In various splitting functions separate pieces can be angular ordered and anti-ordered
 - There is always a regular contribution. **Neither of the 5 branchings is angular ordered**
 - The angular-ordering ansatz is in direct contradiction to this results
- $q \rightarrow \bar{q}'q'\bar{q}, q \rightarrow \bar{q}qq, q \rightarrow ggq,$
 $g \rightarrow gq\bar{q}, g \rightarrow ggg$

Feynman graphs for the q->ggq splitting in dense QCD matter

- SCET with Glauber gluons, hybrid gauge



- We checked every Feynman diagram by comparing analytical calculation with FeynCalc

Form of an arbitrary diagram

Single Born:

$$A_k^{(1)} = -g^2 \varepsilon_1^{i_1} \varepsilon_2^{i_2} \bar{\chi}_{n,p} \left(\int d\Phi_{\perp} C_k \Gamma_k^{i_1 i_2} I_k^{(1)} \right) J,$$

Double Born:

$$A_k^{(2c)} = g^2 \varepsilon_1^{i_1} \varepsilon_2^{i_2} \bar{\chi}_{n,p} \left(\int d\Phi_{1\perp} d\Phi_{2\perp} C_k \Gamma_k^{i_1 i_2} I_k^{(2c)} \right) J,$$

Coefficient

Lorentz structure

Longitudinal integral

- Coefficients C_k are overall coefficients that depend on the diagram
- Lorentz structure directly follows from rules of **SCET_G**, includes a vector in the color space
- Longitudinal integrals are same as those that appear in **GLV**

Single Born (19)

k	C_k	$\mathbf{U}_{p_{k_1}, p_{k_2}}^{j_1} \mathbf{U}_{p_{k_3}, p_{k_4}}^{j_2}$	$I_k^{(1)}$
1	$1/s_{123}$	—	$I_1(\Omega_0)$
2	$1/\bar{n} \cdot p_0$	—	$I_2(\Omega_0, \Omega_2)$
3	$1/\bar{n} \cdot p_0$	—	$I_2(\Omega_0, \Omega_1)$
4	$1/\bar{n} \cdot p_0$	—	$I_2(\Omega_0, \Omega_3)$
5	$1/s_{13}s_{123}$	$\mathbf{U}_{k_1, p}^{j_1} \mathbf{U}_{k_2, p+k_1}^{j_2}$	$I_1(\Omega_0)$
6	$1/\bar{n} \cdot p_0 s_{13}$	$\mathbf{U}_{k_1, p}^{j_1} \mathbf{U}_{k_2, p+k_1}^{j_2}$	$I_2(\Omega_0, \Omega_2)$
7	$1/(\bar{n} \cdot p_0)^2(z_1 + z_3)$	$\mathbf{U}_{k_1-q, p}^{j_1} \mathbf{U}_{k_2, p+k_1-q}^{j_2}$	$I_3(\Omega_0, \Omega_1, \Omega_5)$
8	$1/(\bar{n} \cdot p_0)^2(z_1 + z_3)$	$\mathbf{U}_{k_1-p, q}^{j_1} \mathbf{U}_{k_2, p-q+k_1}^{j_2}$	$I_3(\Omega_0, \Omega_3, \Omega_5)$
9	$1/\bar{n} \cdot p_0 s_{13}$	$\mathbf{U}_{k_1, p}^{j_1} \mathbf{U}_{k_2, p+k_1-q}^{j_2}$	$I_2(\Omega_0, \Omega_5)$
10	$1/s_{23}s_{123}$	$\mathbf{U}_{k_2, p}^{j_1} \mathbf{U}_{k_1, p+k_2}^{j_2}$	$I_1(\Omega_0)$
11	$1/\bar{n} \cdot p_0 s_{23}$	$\mathbf{U}_{k_2, p}^{j_1} \mathbf{U}_{k_1-q, p+k_2}^{j_2}$	$I_2(\Omega_0, \Omega_1)$
12	$1/(\bar{n} \cdot p_0)^2(z_2 + z_3)$	$\mathbf{U}_{k_2-q, p}^{j_1} \mathbf{U}_{k_1, p+k_2-q}^{j_2}$	$I_3(\Omega_0, \Omega_2, \Omega_4)$
13	$1/(\bar{n} \cdot p_0)^2(z_2 + z_3)$	$\mathbf{U}_{k_2-p, q}^{j_1} \mathbf{U}_{k_1, p-q+k_2}^{j_2}$	$I_3(\Omega_0, \Omega_3, \Omega_4)$
14	$1/\bar{n} \cdot p_0 s_{23}$	$\mathbf{U}_{k_2, p}^{j_1} \mathbf{U}_{k_1, p+k_2-q}^{j_2}$	$I_2(\Omega_0, \Omega_4)$
15	$1/s_{12}s_{123}$	$\mathbf{U}_{k_1, k_2}^{j_1} \mathbf{U}_{k_1+k_2, p}^{j_2}$	$I_1(\Omega_0)$
16	$1/(\bar{n} \cdot p_0)^2(z_1 + z_2)$	$\mathbf{U}_{k_1, k_2-q}^{j_1} \mathbf{U}_{k_1+k_2, p-q}^{j_2}$	$I_3(\Omega_0, \Omega_2, \Omega_6)$
17	$1/(\bar{n} \cdot p_0)^2(z_1 + z_2)$	$\mathbf{U}_{k_1-q, k_2}^{j_1} \mathbf{U}_{k_1-q+k_2, p}^{j_2}$	$I_3(\Omega_0, \Omega_1, \Omega_6)$
18	$1/\bar{n} \cdot p_0 s_{12}$	$\mathbf{U}_{k_1, k_2}^{j_1} \mathbf{U}_{k_1+k_2, p-q}^{j_2}$	$I_2(\Omega_0, \Omega_3)$
19	$1/\bar{n} \cdot p_0 s_{12}$	$\mathbf{U}_{k_1, k_2}^{j_1} \mathbf{U}_{k_1+k_2-q, p}^{j_2}$	$I_2(\Omega_0, \Omega_6)$

Table 1: Entries for single Born graphs.

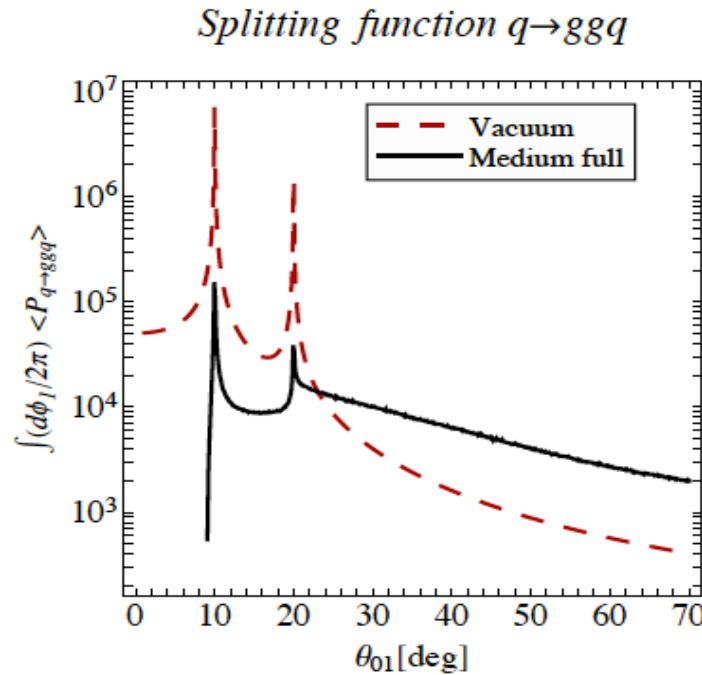
Double Born (34)

k	C_k	$\mathbf{U}_{p_{k_1}, p_{k_2}}^{j_1} \mathbf{U}_{p_{k_3}, p_{k_4}}^{j_2}$	$I_k^{(2c)} / (-i)$
1	$1/s_{123}$	—	$I_1(\Omega_0)/2$
2	$1/\bar{n} \cdot p_0$	—	$I_2(\Omega_0, \Omega_2)/2$
3	$1/\bar{n} \cdot p_0$	—	$I_2(\Omega_0, \Omega_1)/2$
4	$1/\bar{n} \cdot p_0$	—	$I_2(\Omega_0, \Omega_3)/2$
5	$1/\bar{n} \cdot p_0$	—	$I_2(\Omega_0, \Omega_2 + \Omega_3)$
6	$1/\bar{n} \cdot p_0$	—	$I_2(\Omega_0, \Omega_1 + \Omega_3)$
7	$1/\bar{n} \cdot p_0$	—	$I_2(\Omega_0, \Omega_2 + \Omega_1)$
8	$1/s_{13}s_{123}$	$\mathbf{U}_{k_1, p}^{j_1} \mathbf{U}_{k_2, p+k_1}^{j_2}$	$I_1(\Omega_0)/2$
9	$1/\bar{n} \cdot p_0 s_{13}$	$\mathbf{U}_{k_1, p}^{j_1} \mathbf{U}_{k_2, p+k_1}^{j_2}$	$I_2(\Omega_0, \Omega_2)/2$
10	$1/(\bar{n} \cdot p_0)^2(z_1 + z_3)$	$\mathbf{U}_{k_1, p}^{j_1} \mathbf{U}_{k_2, p+k_1}^{j_2}$	$I_3(\Omega_0, \Omega_1, \Omega_5)/2$
11	$1/(\bar{n} \cdot p_0)^2(z_1 + z_3)$	$\mathbf{U}_{k_1, p}^{j_1} \mathbf{U}_{k_2, p+k_1}^{j_2}$	$I_3(\Omega_0, \Omega_3, \Omega_5)/2$
12	$1/\bar{n} \cdot p_0 s_{13}$	$\mathbf{U}_{k_1, p}^{j_1} \mathbf{U}_{k_2, p+k_1}^{j_2}$	$I_2(\Omega_0, \Omega_5)/2$
13	$1/(\bar{n} \cdot p_0)^2(z_1 + z_3)$	$\mathbf{U}_{k_1-p, q}^{j_1} \mathbf{U}_{k_2, p-q+k_1}^{j_2}$	$I_3(\Omega_0, \Omega_2 + \Omega_3, \Omega_2 + \Omega_5)$
14	$1/(\bar{n} \cdot p_0)^2(z_1 + z_3)$	$\mathbf{U}_{k_1-q, p}^{j_1} \mathbf{U}_{k_2, p+k_1}^{j_2}$	$I_3(\Omega_0, \Omega_5, \Omega_1 + \Omega_3)$
15	$1/(\bar{n} \cdot p_0)^2(z_1 + z_3)$	$\mathbf{U}_{k_1-q, p}^{j_1} \mathbf{U}_{k_2+q, p+k_1-q}^{j_2}$	$I_3(\Omega_0, \Omega_2 + \Omega_1, \Omega_2 + \Omega_5)$
16	$1/\bar{n} \cdot p_0 s_{13}$	$\mathbf{U}_{k_1, p}^{j_1} \mathbf{U}_{k_2+q, p+k_1-q}^{j_2}$	$I_2(\Omega_0, \Omega_5 + \Omega_2)$
17	$1/s_{23}s_{123}$	$\mathbf{U}_{k_2, p}^{j_1} \mathbf{U}_{k_1, p+k_2}^{j_2}$	$I_1(\Omega_0)/2$
18	$1/\bar{n} \cdot p_0 s_{23}$	$\mathbf{U}_{k_2, p}^{j_1} \mathbf{U}_{k_1, p+k_2}^{j_2}$	$I_2(\Omega_0, \Omega_1)/2$
19	$1/(\bar{n} \cdot p_0)^2(z_2 + z_3)$	$\mathbf{U}_{k_2, p}^{j_1} \mathbf{U}_{k_1, p+k_2}^{j_2}$	$I_3(\Omega_0, \Omega_2, \Omega_4)/2$
20	$1/(\bar{n} \cdot p_0)^2(z_2 + z_3)$	$\mathbf{U}_{k_2, p}^{j_1} \mathbf{U}_{k_1, p+k_2}^{j_2}$	$I_3(\Omega_0, \Omega_3, \Omega_4)/2$
21	$1/\bar{n} \cdot p_0 s_{23}$	$\mathbf{U}_{k_2, p}^{j_1} \mathbf{U}_{k_1, p+k_2}^{j_2}$	$I_2(\Omega_0, \Omega_4)/2$
22	$1/(\bar{n} \cdot p_0)^2(z_2 + z_3)$	$\mathbf{U}_{k_2, p}^{j_1} \mathbf{U}_{k_1-q, p+k_1-q}^{j_2}$	$I_3(\Omega_0, \Omega_1 + \Omega_4, \bar{\Omega}_1 + \Omega_3)$
23	$1/(\bar{n} \cdot p_0)^2(z_2 + z_3)$	$\mathbf{U}_{k_2-q, p}^{j_1} \mathbf{U}_{k_1+p, k_2}^{j_2}$	$I_3(\Omega_0, \Omega_4, \Omega_2 + \Omega_3)$
24	$1/(\bar{n} \cdot p_0)^2(z_2 + z_3)$	$\mathbf{U}_{k_2-q, p}^{j_1} \mathbf{U}_{k_1+q, p+k_2-q}^{j_2}$	$I_3(\Omega_0, \Omega_1 + \Omega_2, \Omega_1 + \bar{\Omega}_4)$
25	$1/\bar{n} \cdot p_0 s_{23}$	$\mathbf{U}_{k_2-q, p}^{j_1} \mathbf{U}_{k_1+q, p+k_2-q}^{j_2}$	$I_2(\Omega_0, \Omega_4 + \Omega_1)$
26	$1/s_{12}s_{123}$	$\mathbf{U}_{k_1, k_2}^{j_1} \mathbf{U}_{k_1+k_2, p}^{j_2}$	$I_1(\Omega_0)/2$
27	$1/(\bar{n} \cdot p_0)^2(z_1 + z_2)$	$\mathbf{U}_{k_1, k_2}^{j_1} \mathbf{U}_{k_1+k_2, p}^{j_2}$	$I_3(\Omega_0, \Omega_2, \Omega_6)/2$
28	$1/(\bar{n} \cdot p_0)^2(z_1 + z_2)$	$\mathbf{U}_{k_1, k_2}^{j_1} \mathbf{U}_{k_1+k_2, p}^{j_2}$	$I_3(\Omega_0, \Omega_1, \Omega_6)/2$
29	$1/\bar{n} \cdot p_0 s_{12}$	$\mathbf{U}_{k_1, k_2}^{j_1} \mathbf{U}_{k_1+k_2, p}^{j_2}$	$I_2(\Omega_0, \Omega_3)/2$
30	$1/\bar{n} \cdot p_0 s_{12}$	$\mathbf{U}_{k_1, k_2}^{j_1} \mathbf{U}_{k_1+k_2, p}^{j_2}$	$I_2(\Omega_0, \Omega_6)/2$
31	$1/(\bar{n} \cdot p_0)^2(z_1 + z_2)$	$\mathbf{U}_{k_1-q, k_2}^{j_1} \mathbf{U}_{k_1-k_2+q, p+q}^{j_2}$	$I_3(\Omega_0, \Omega_3 + \Omega_2, \Omega_3 + \Omega_6)$
32	$1/(\bar{n} \cdot p_0)^2(z_1 + z_2)$	$\mathbf{U}_{k_1-k_2-q}^{j_1} \mathbf{U}_{k_1+k_2-q, p+q}^{j_2}$	$I_3(\Omega_0, \Omega_3 + \Omega_1, \Omega_3 + \Omega_6)$
33	$1/(\bar{n} \cdot p_0)^2(z_1 + z_2)$	$\mathbf{U}_{k_1-q, k_2+q}^{j_1} \mathbf{U}_{k_1+k_2, p-q}^{j_2}$	$I_3(\Omega_0, \Omega_6, \Omega_1 + \Omega_2)$
34	$1/\bar{n} \cdot p_0 s_{12}$	$\mathbf{U}_{k_1, k_2}^{j_1} \mathbf{U}_{k_1+k_2-q, p+q}^{j_2}$	$I_2(\Omega_0, \Omega_3 + \Omega_6)$

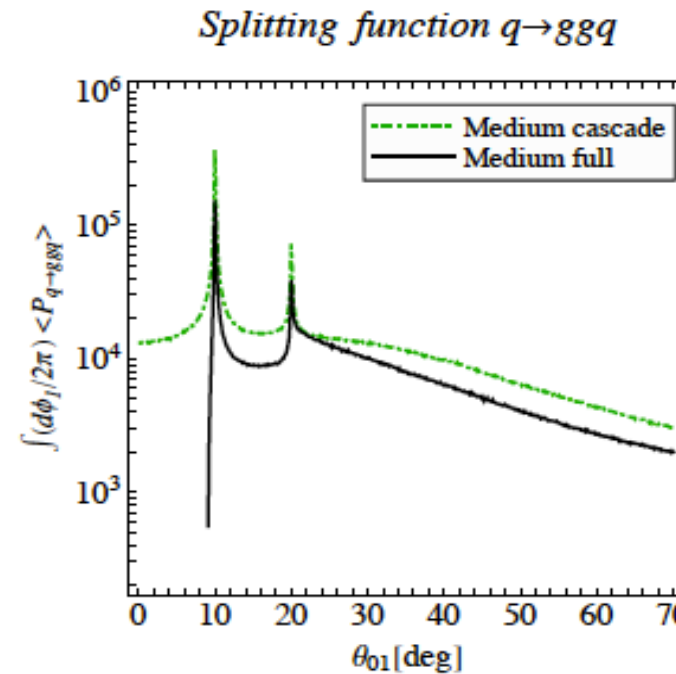
Table 2: Entries for double Born graphs.

Benchmark result

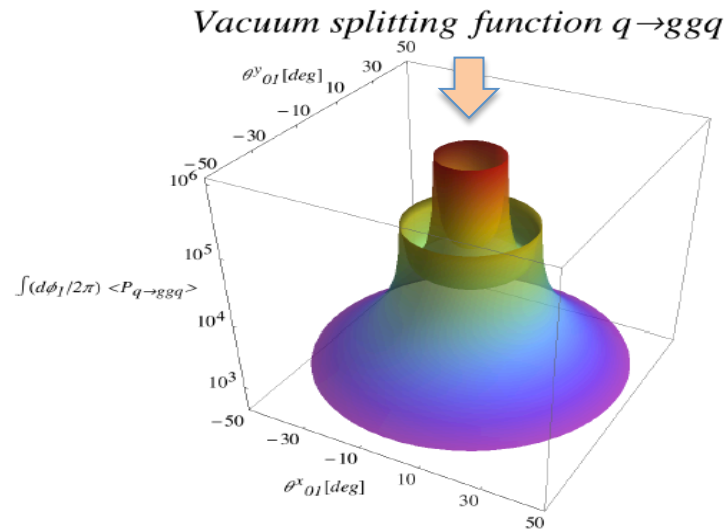
- The medium splitting function is much broader than the vacuum one. It falls off less steeply in parts of the tail region
- Medium cascade works reasonably well in the tail region in shape. Norm is off by a factor of 2. Along the original direction it does not get the LPM cancellation
- The splitting functions are not angular ordered or angular anti-ordered
- Full result for the splitting function compared to analytic simplified result valid in small z_1 limit, are indistinguishable on this plot



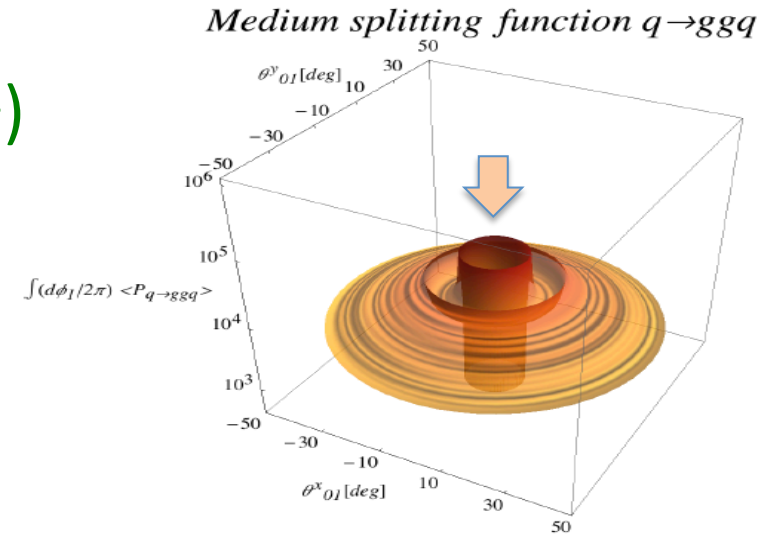
$$z_1 = 0.03 \quad z_2 = 2/3 \quad \theta_{20} = 10^\circ, \theta_{30} = 20^\circ$$



An complementary view

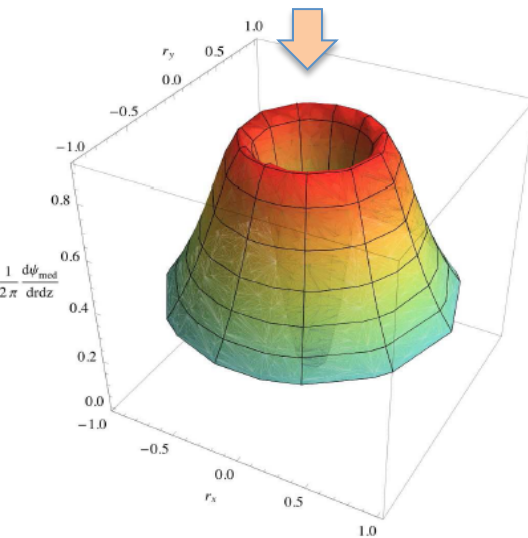


$$O(\alpha_s^2)$$

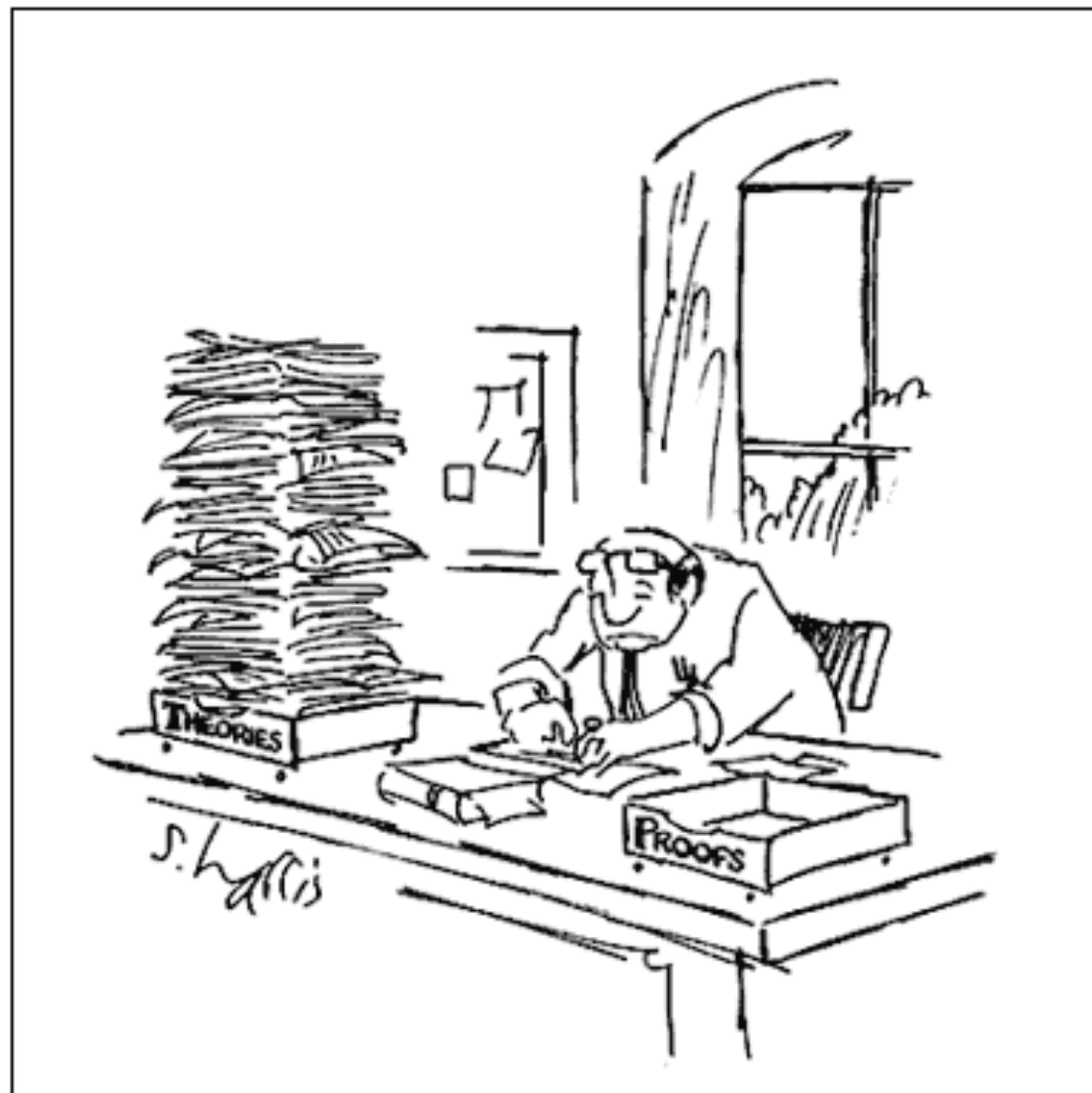


$$O(\alpha_s)$$

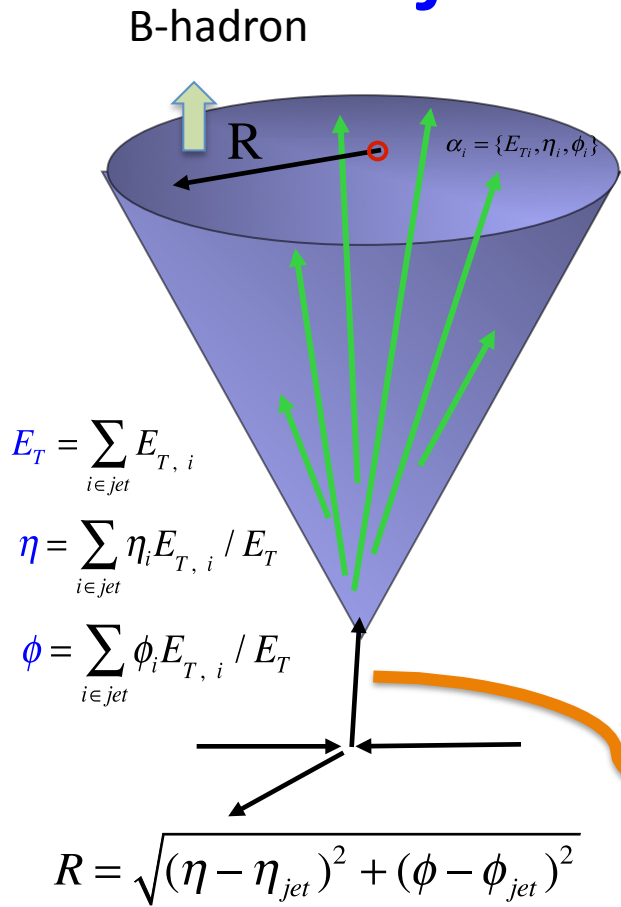
- Note that the cancellation in the center arises from the LPM effect for jets produced in hard scattering process. This is the also case for the lowest order splitting



III. B-jet production in HIC



B-jets and their ambiguity



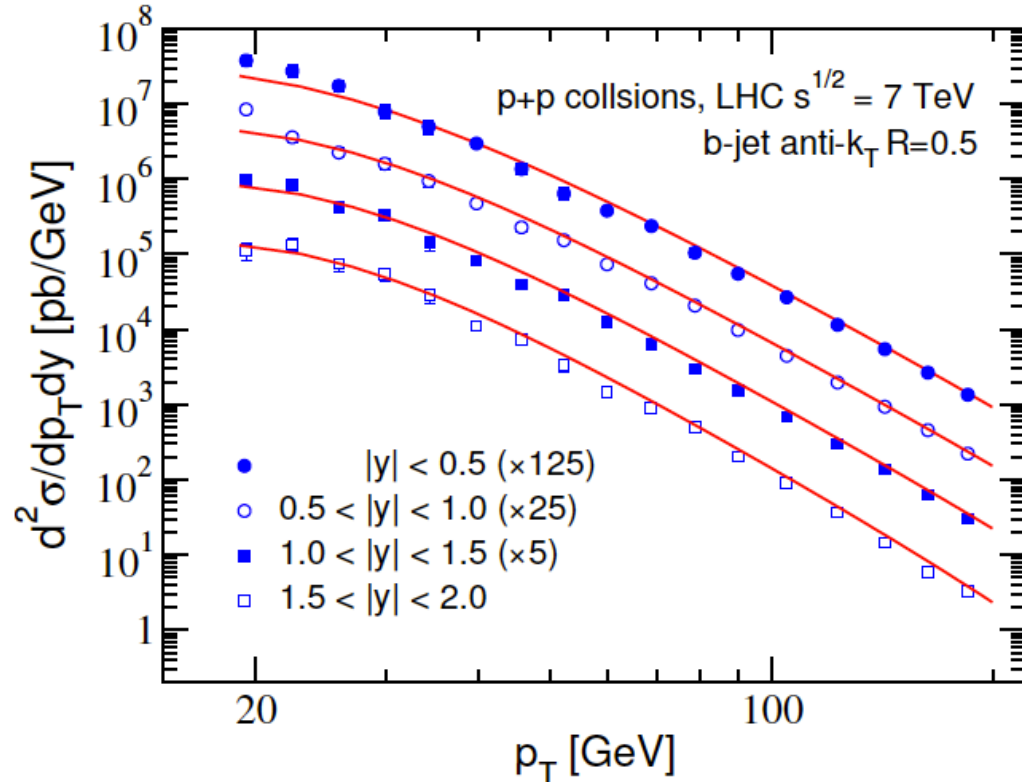
- Jet finding algorithms [have to satisfy collinear and infrared safety]:
 - 1) Successive recombination algorithms
 - a) k_t algorithm S. Ellis et al. (1993)
 - b) anti- k_t algorithm
 - 2) Iterative cone algorithms:
 - a) cone algorithm with “seed”: CDF, D0
 - b) “seedless” cone algorithm
 - c) midpoint cone algorithm G. Salam et al. (2007)

Note that the parent parton has little to do with a b-quark
- First find a jet. Next, with the jet radius parameter look for a b-hadron (b-quark for theory). Call it a b-jet Or maybe require the b-quark to be leading ... Or maybe some more creative substructure approach ...

B-jets as they are being done today

- No readily available NLO calculation for b-jet production
- Pythia 8 (LO + LL parton shower)
- SlowJet program with an anti- k_T algorithm (versus FastJet) shown to give the same result

Studied the hadronization corrections. Only important for $p_T < 30$ GeV and $R = 0.2, 0.3$. Consistent with the ideas in the original “Snowmass accord”

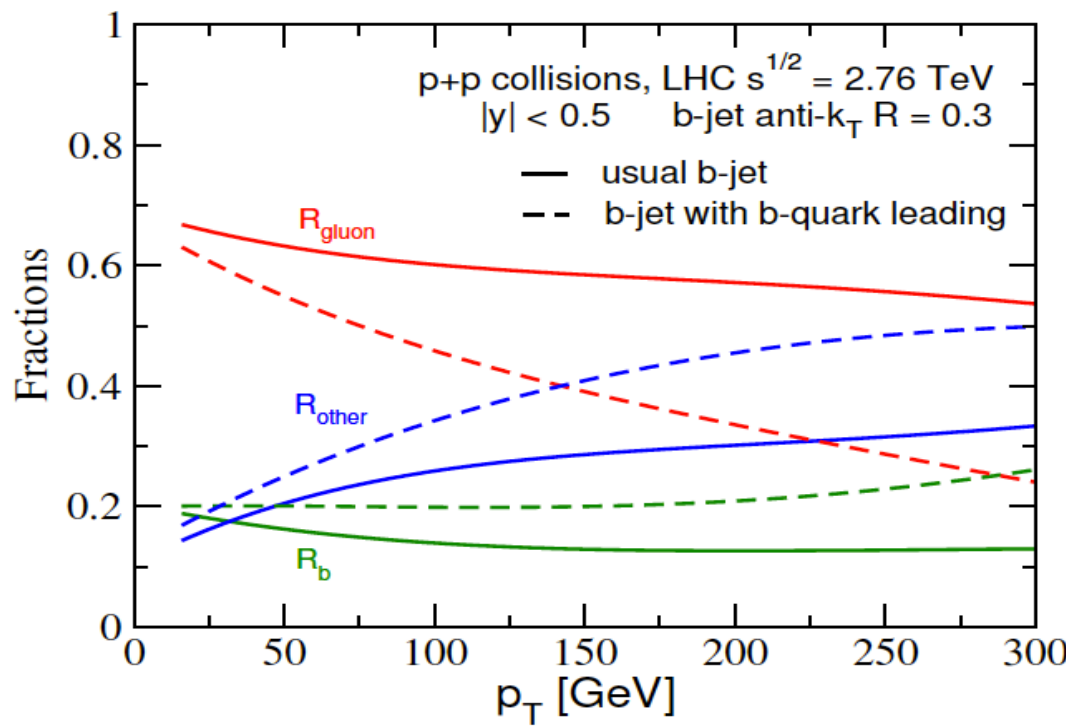


Chatrchyan et al. (2012)

- Good comparison to the b-jet cross sections versus p_T and rapidity y

Hard partonic structure for b-jets

- Evaluated both **initial-state** (for CNM effects, **small**) and **final-state** partonic fraction (for the quenching, **large**)



Evaluated in the fixed flavor number scheme

- R_{gluon} - fraction of $g \rightarrow b(\bar{b})$
- R_{other} - fraction of $q(\bar{q}) \rightarrow b(\bar{b})$
- R_b - fraction of $b(\bar{b}) \rightarrow b(\bar{b})$

A very small fraction of B-jets originate form a b-quark produced in the hard scattering. The “mix” is similar to light jets

Evaluating the energy loss of jets

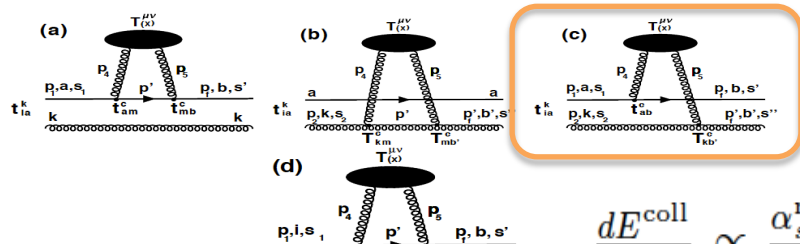
To discuss radiative “energy loss” the calculation must be done in the soft gluon approximation

- Radiative energy loss: works by transporting the energy outside of the cone through large-angle medium induced bremsstrahlung

$$\Delta E_{\text{LPM suppressed}}^{\text{rad}} \Rightarrow \frac{dI^g}{d\omega}(\omega \sim E)_{\text{LPM suppressed}}$$

$$\Rightarrow \frac{dI^g}{d\omega d^2 k_T}(k_T \ll \omega)_{\text{LPM suppressed}} \sim \frac{dI^g}{d\omega dr}(r \ll R)_{\text{suppressed}}$$

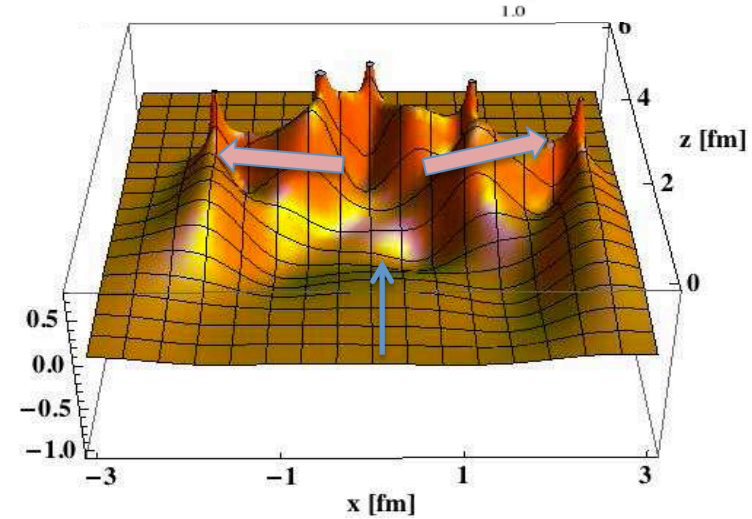
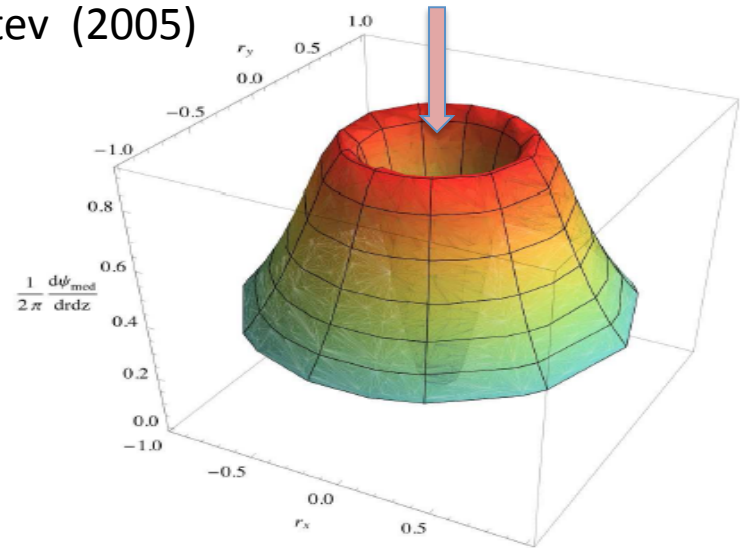
- Collisional energy loss: works by thermalizing the soft(ish) modes and transporting them away from the jet axis



R.B. Neufeld,
I. Vitev (2011)

$$\frac{dE^{\text{coll}}}{d\Delta z} \propto \frac{\alpha_s^{\text{med}} C_{(s)} m_D^2}{2} \ln \frac{\sqrt{ET}}{m_D},$$

I. Vitev (2005)

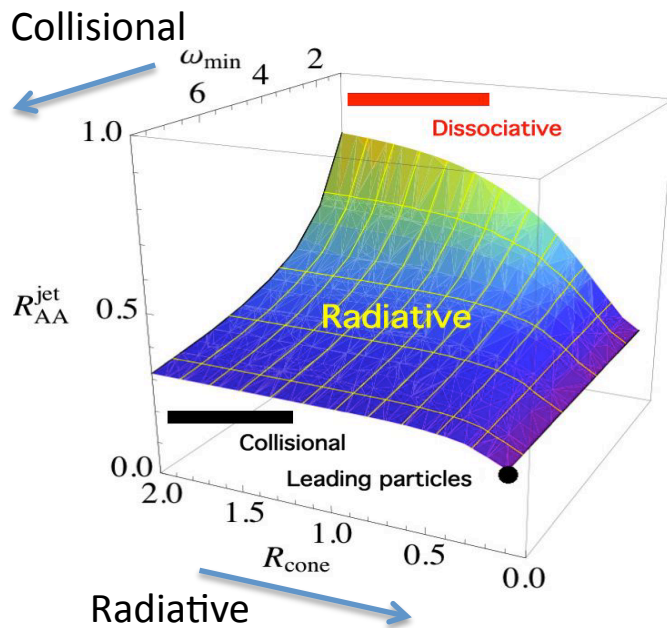


Exploring the energy loss mechanisms

- Exploiting the jet variables in heavy ion collisions (R)
- Making use of intrajet observables (e.g. ψ)

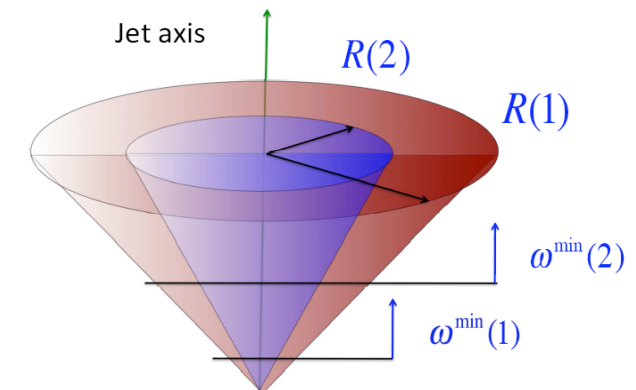
I.Vitev., S.Wicks, B.W.Zhang (2008)

- Qualitative expectations (how to interpret the experimental results)



$$R_{AA}^{jet}(E_T; R^{\max}, \omega^{\min}) = \frac{\frac{d\sigma^{AA}(E_T; R^{\max}, \omega^{\min})}{dy d^2 E_T}}{\langle N_{\text{bin}} \rangle \frac{d\sigma^{pp}(E_T; R^{\max}, \omega^{\min})}{dy d^2 E_T}}$$

Mechanism	Signature	Status
Radiative	Continuous variation of R_{AA}^{jet} with R	<ul style="list-style-type: none"> ✓ Incl. jets at RHIC, LHC ✓ Di-jets at the LHC ✓ Z^0-, γ-tagged jets ✓ B-jets
Collisional	\sim Constant $R_{AA}^{jet} = R_{AA}^{\text{particle}}$ (Large suppression)	<ul style="list-style-type: none"> ✓ Incl. jets at LHC ✓ Di-jets at the LHC ✓ Z^0-, γ-tagged jets ✓ B-jets



Evaluating the jet cross section

- Only a fraction of lost energy (medium induced parton shower) falls **inside** the cone and is **not** dissipated due to collisional interactions

$$\frac{1}{\langle N_{\text{bin}} \rangle} \frac{d^2\sigma_{AA}^{\text{b-jet}}(R)}{dydp_T} = \sum_{(s)} \int_0^1 d\epsilon \frac{P_{(s)}(\epsilon)}{(1 - [1 - f(R, \omega^{\text{coll}})_{(s)}]\epsilon)}$$

$$\times \frac{d^2\sigma_{(s)}^{\text{CNM,LO+PS}}(|J(\epsilon)|_{(s)} p_T)}{dydp_T}$$

- The fraction that is inside the cone (**1-f is lost**)

$$f(R, \omega^{\text{coll}})_{(s)} = \frac{\int_0^R dr \int_{\omega^{\text{coll}}}^E d\omega \frac{\omega d^2 N_{(s)}^g}{d\omega dr}}{\int_0^{R^\infty} dr \int_0^E d\omega \frac{\omega d^2 N_{(s)}^g}{d\omega dr}}$$

$$f(R^\infty, \omega^{\text{coll}})_{(s)} = \Delta E^{\text{coll}}/E$$

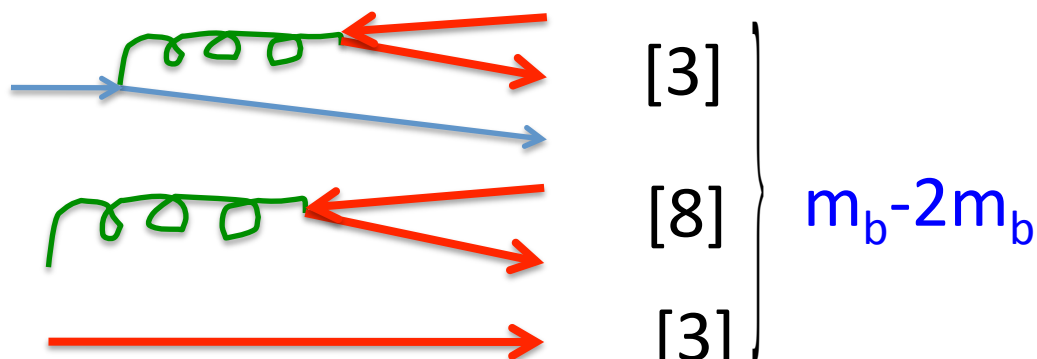
- Higher energy needed due to energy loss:

$$E'_T = E_T / (1 - (1 - f_{q,g}) \cdot \epsilon)$$

This is by now fairly standard. The real question is what are the states (s) that propagate through the QGP

Guidance from quarkonium production

- At high transverse momenta quarkonium production is dominated by a color-octet mechanism. Quenching of an effective gluon state with mass $2m_b$ starts to kick in at high p_T
- The states for b-jet production



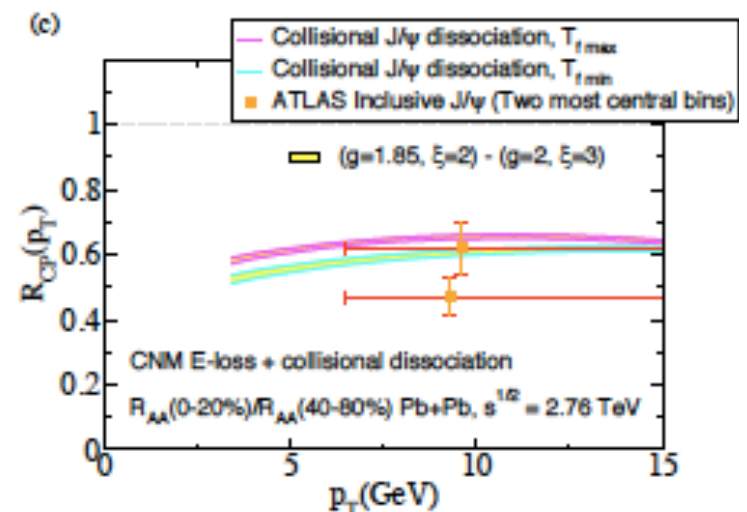
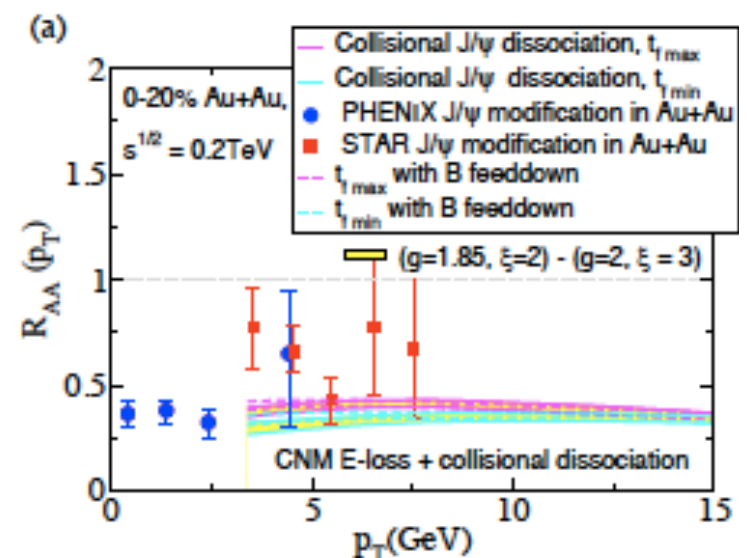
Mass and thermal effects (propagators and interference phases)

M. Djordjevic,

M. Gyulassy (2004)

$$\mathbf{k}^2 \rightarrow \mathbf{k}^2 + x^2 M^2$$

$$\mathbf{k}^2 \rightarrow \mathbf{k}^2 + m_D^2$$

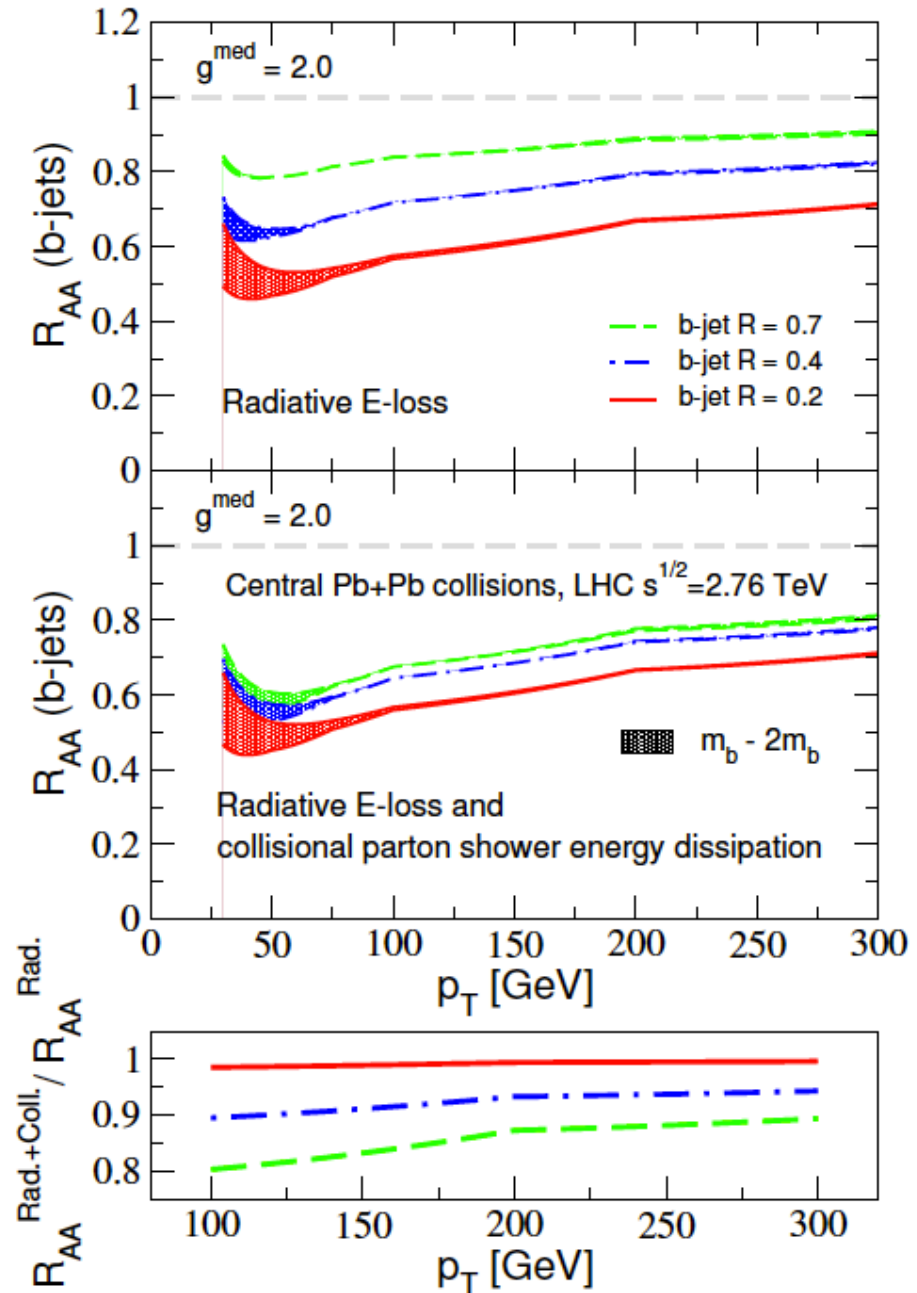


R. Sharma, I.Vitev. (2012)

B-jet results

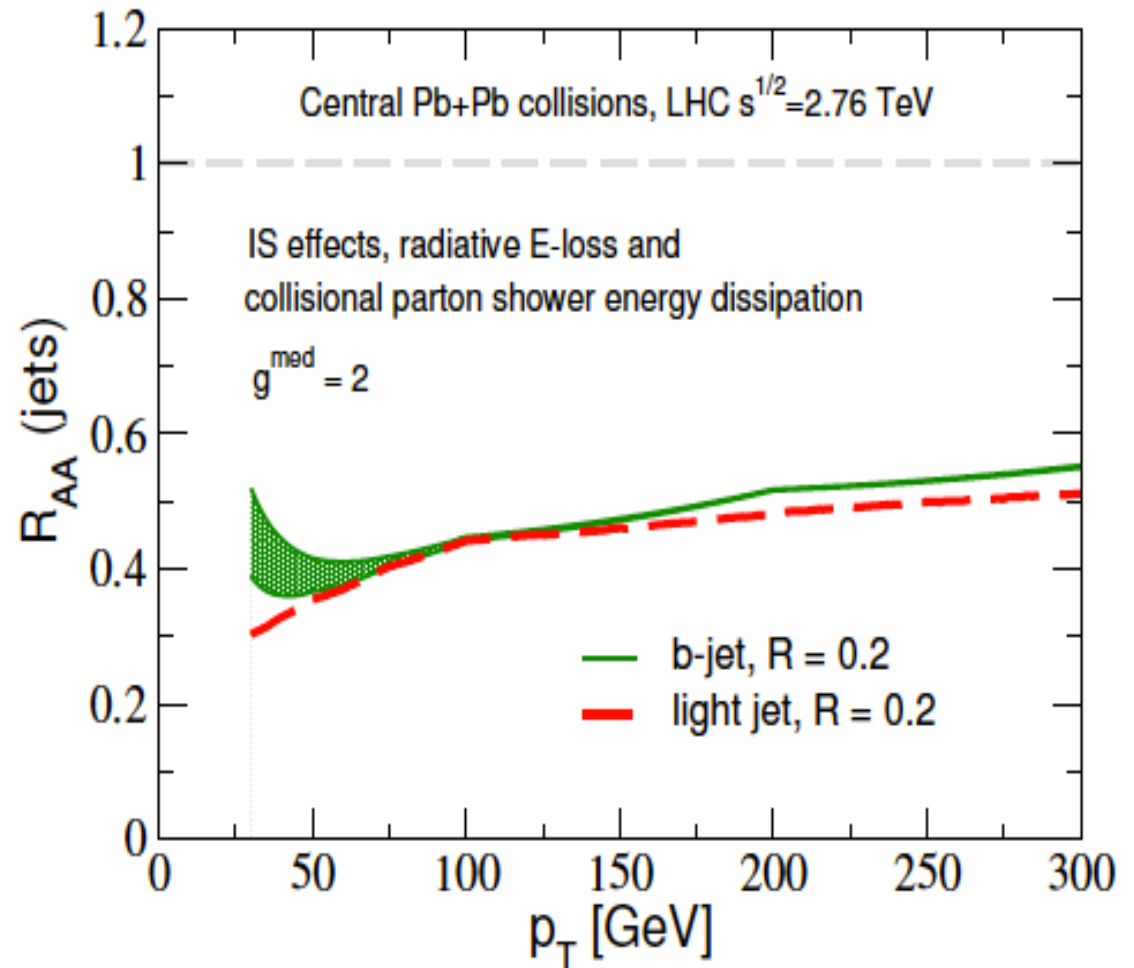
Phenomenology suitable for direct comparison to the 2.76 TeV LHC results

- For radiative energy loss only, the R dependence is clearly visible.
- With collisional energy loss, this R dependence is reduced
- The collisional energy loss contribution is 30% to 50%. It is less than for light jets due to a less populated medium-induced parton shower

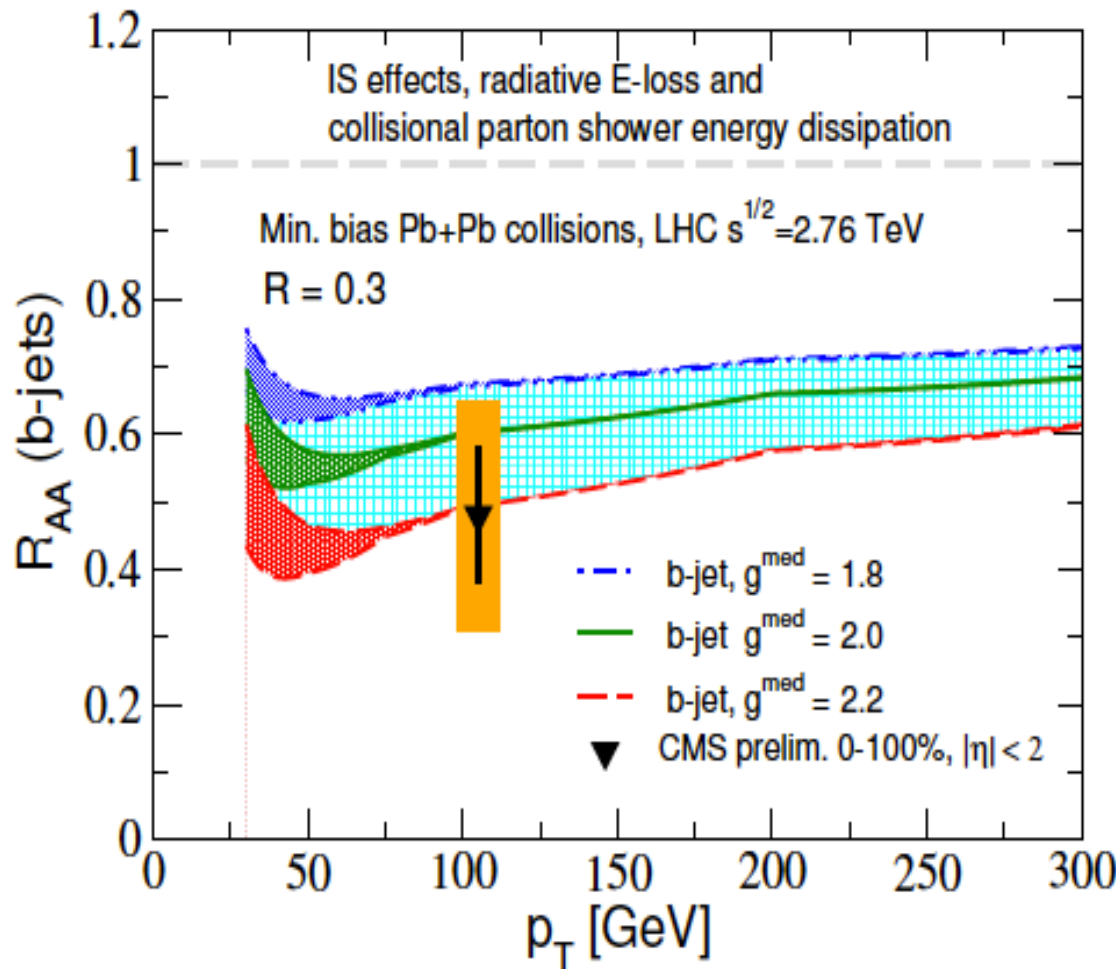


Direct comparison between b-jets and light jets

- At high p_T the suppression of b-jets is very very similar to that of light jets
(The minor difference on this figure is less than the uncertainty in the simulations)
The light jet simulation is 3Y old
- At $p_T < 50$ GeV the difference is due to the mass effect



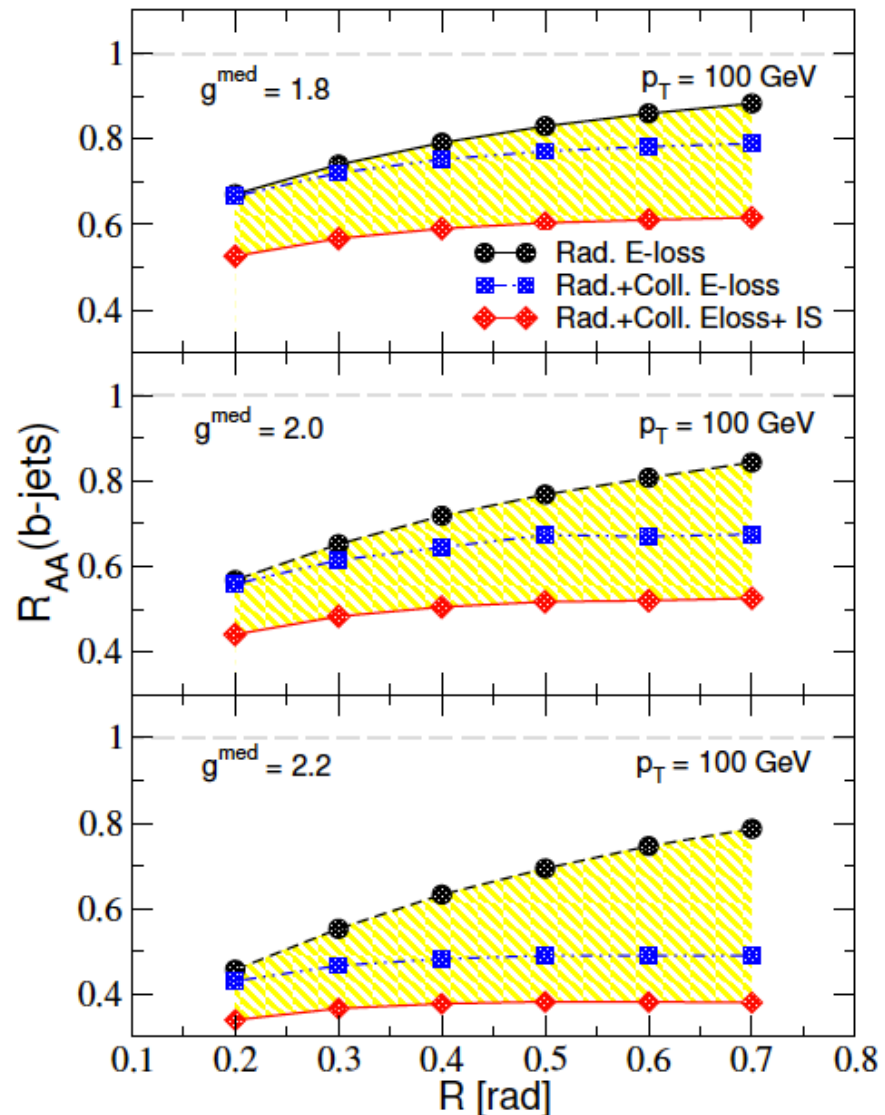
Comparison to preliminary CMS data



- Agreement in the large error bars for the couplings that have worked for inclusive and tagged jets ($g=2$, $g = 2.2$)
- Even though this does not look so puzzling any more it is very important. It is a demonstration that E-loss regime is the coherent LPM regime (Where mass dependence disappears).
- If one looks for the actual mass effects (or wants to make a case for the measurement), this is at lower $p_T < 50$ GeV (of jets can be reliably reconstructed)

Differential jet radius studies

- CNM energy loss plays an important role only for small jet-medium couplings ($g=1.8$), which are disfavored anyway
- CNM to be constrained in p+A collisions. One expects $\sim 7.5\%$
- The slope of the R_{AA} vs the jet radius R can be related to the relative contribution of collisional and radiative E-losses



Conclusions

- For the majority of the observables that we study today semi-analytic calculations of jet production ($p+p$ and $A+A$) work well. There is no sensitivity to poorly controlled hadronization effects.
- We developed the gauge sector of $SCET_G$, which allowed to significantly advance the understanding of the in-medium parton shower formation (phenomenology to come soon).
- We studied the angular distributions of *collinear* (valid at the parton shower distance scale) splitting functions in the vacuum and in dense QCD matter. First derivation to $O(\alpha_s^2)$ in the medium
- In all cases we found that the full splitting functions are neither angular ordered nor anti-ordered. Helps understand the success of the jet production calculations for observables of interest.
- The main features are the broader angular distribution and the cancellation on the center, first found to $O(\alpha_s^2)$
- Performed the first calculation for b-jets. We studied what are the effective states that propagate through the QGP motivated by our work on quarkonia at high p_T .
- At high p_T the suppression of b-jets is very similar to that of light jets. This is an important result (demonstrates the coherent LPM E-loss regime). The place to look for explicit mass effects is below 50 GeV.